GENETICALLY ACCURATE MODELS OF SOD1-BASED ALS IN *DROSOPHILA MELANOGASTER*

by

Pınar Deniz

B.Sc., Chemical Engineering, Yıldız Technical University, 2008

Submitted to the Institute for Graduate Studies in
Science and Engineering in partial fulfillment of
the requirements for the degree of
Master of Science

Graduate Program in Molecular Biology and Genetics
Boğaziçi University

2011

To my grandmothers

Nevzat Döşoğlu & Gülhan Deniz

and

to my grandfathers

Mehmet Baki Deniz & Adil Döşoğlu

ACKNOWLEDGEMENTS

I would like to express my sincere gratitude to my supervisor Prof. A Nazlı Başak for evaluating my eagerness in MB&G at our first meeting and for giving me the opportunity to be a part of NDAL. Under Prof. Başak‘s guidance, I have learned many things not only in my research field, but also in many others that have enriched me in all aspects.

I would like to extend my thanks to Assoc. Prof. Esra Battaloğlu for her support at the very beginning of my master education and also for her contributions to my thesis. I would also like to express my thanks to Prof. Robert A. Reenan for his precious assistance and for his stimulating ideas on this study as well as for his hospitality during my 3-months stay in his lab. At this point, I would also like to acknowledge Suna-İnan Kıraç Foundation for the financial support it provided throughout my study.

I am endlessly grateful to my dearest fiancé B. Arman Aksoy, for his unbelievable support and presence despite the thousands of miles between us. His patience, scientific and general advices meant a lot to me.

I would also like to acknowledge my “fellow traveler” Gönenç Çobanoğlu. He has been on my side since our college years and throughout these years I had overcome many problems by his support. I would like to thank Dr. İzzet Enünlü for his encouragement and guidance during my studies, and also extend my thanks to Dr. Mehmet Ozansoy, Özgün Uyan, Yetiş Gültekin, Ceren İskender, Ece Kara, Kadir Özkan, Suna Lahut, Dr. Aslıhan Özoğuz, Sercan Sayın, Özgür Ömür, Sena Ağım, Selda Dığın, İlknur Yıldız, Irmak Şahbaz, Aslı Eken and to Reenan Lab members Dr. Maloney, Dr. Savva and Ryan Bell.

Finally, I would like to express my deepest gratitude and love to my whole family. Their presence has been a constant source of love, concern, support and strength from the beginning of my life.

ABSTRACT

GENETICALLY ACCURATE MODELS OF SOD1-BASED ALS IN *DROSOPHILA MELANOGASTER*

ALS is a late onset, rapidly progressive and ultimately fatal neurodegenerative disease, caused by the loss of motor neurons in the brain and spinal cord. Generally, 5-10% of ALS patients have a family history (fALS), whereas there is no apparent genetic contribution for the remaining portion (sALS). Mutations in the SOD1 gene are responsible for 20% of fALS cases. Upon finding of the link between SOD1 mutations and ALS, researchers have begun to generate animal models based on different mSOD1-mediated ALS. Among various animal models, fruit flies stand out as an attractive model organism for studying neurodegenerative diseases with their small, yet still complex brains and also with their many advantages for being appropriate laboratory animals *e.g.* being small and cheap, having short reproductive and developmental cycles etc. Homologous recombination can be used for introducing disease-causing human mutations into endogenous *Drosophila* genes. Because endogenous gene regulation remains intact by this method, mutations introduced into endogenous *Drosophila* genes may provide accurate genetic models of disease. The aim of this thesis was to establish the methodology of HR using *Drosophila* as a model system at Bogazici University, NDAL laboratory in collaboration with Robert Reenan laboratory at Brown University. The specific aim of this study was to introduce two different ALS-linked human SOD1-mutations (G37R and H48R) into *Drosophila* dSOD gene. Within this study, these two mutations were successfully inserted into the dSOD gene. After backcrossing of the mutant lines to wild type line for sufficient generations in order to minimize background effects, these G37R and H48R mutant flies can be used as model organisms in ALS research.

ÖZET

SOD1 KAYNAKLI ALS'NİN *DROZOFİLA MELANOGASTER*'DA GENETİK AÇIDAN DOĞRU ŞEKİLDE MODELLENMESİ

ALS, beyin ve omurilikteki motor nöronların kaybından kaynaklanan, geç başlangıçlı, hızlı ilerleyen ve ölümle sonuçlanan nörodejeneratif bir hastalıktır. Genellikle, ALS hastalarının %5-10 kadarının bilinen ailesel bir hastalık geçmişi varken (fALS), hastaların geriye kalan kısmında genetiğin rolü belirgin değildir (sALS). fALS hastalığının %20'si, SOD1 geninde bulunan mutasyonlardan kaynaklıdır. SOD1 ve ALS arasındaki ilişkinin anlaşılmasından sonra, araştırmacılar mutant SOD1 kaynaklı ALS için hayvan modelleri geliştirmeye başlamışlardır. Çeşitli hayvan modellerinin arasında meyve sinekleri, küçük fakat aynı zamanda karmaşık beyin yapıları ve laboratuvar ortamında sağladıkları kolaylıklar (küçük olmaları, bakımlarının ucuz olması, üreme ve gelişme döngülerinin kısa sürmesi gibi) sayesinde, nörodejeneratif hastalıkların çalışılmasında cazip hayvan modelleri olarak ön plana çıkmaktadırlar. Homolog rekombinasyon (HR), insanlarda gözlenen hastalık nedeni mutasyonların, endojen *Drozofila* genlerinde modellenmesi için kullanılan bir yöntemdir. Bu yöntemde, endojen genlerin anlatımlarında değişiklik olmadığından, *Drozofila* genlerinde bu yöntemle yaratılan mutasyonlar, hastalıkların doğru bir şekilde modellenmesini sağlar. Bu tez çalışmasının amacı, Brown Üniversitesi'ndeki Robert Reenan laboratuvarı ile ortak yürütülen bir proje çerçevesinde, *Drozofila* modeli üzerinde HR yönteminin NDAL laboratuvarında kurulması ve de bu yöntem kullanılarak, insanlarda gözlenen ALS ile ilişkili iki farklı SOD1 mutasyonunun –G37R ve H48R– *Drozofila*'daki SOD geninde yaratılmasıdır. Bu çalışma çerçevesinde elde edilecek mutant sinekler, arka plan etkilerinin en aza indirilmesi için birkaç nesil, yaban türü sineklerle melezlendikten sonra, ALS çalışmalarında model organizma olarak kullanılabileceklerdir.

TABLE OF CONTENTS

LIST OF FIGURES

LIST OF TABLES

LIST OF ABBREVIATIONS

µg	Microgram
µl	Microliter
µM	Micromolar
AD	Alzheimer's Disease
ALS	Amyotrophic Lateral Sclerosis
ALS2	Alsin
a.m.	Ante Meridiem
AMPA	2-amino-3-(5-methyl-3-oxo-1,2- oxazol-4-yl)propanoic acid
ANG	Angiogenin
Asp	Aspartic Acid
ATP	Adenosine Triphosphate
Bcl-2	B-cell lymphoma 2
bp	Base Pair
BSA	Bovine Serum Albumine
CCS	Copper Chaperone For Superoxide Dismutase
CIP	Calf Intestine Phosphatase
CNS	Central Nervous System
DCTN1	Dynactin 1
Del	Deletion
DNA	Deoxyribonucleic Acid
dNTP	Deoxyribonucleotide Triphosphate
DSB	Double Strand Break
dSOD	Drosophila SOD
EAAT	Excitatory Amino Acid Neurotransmitter
EDTA	Ethylenediaminetetraacetic Acid
ER	Endoplasmic Reticulum
EtBr	Ethidium Bromide
fALS	Familial Amyotrophic Lateral Sclerosis
FLP	Flippase

FTD	Frontotemporal Dementia
FRT	Flippase Recognition Target
FUS/ TLS	Fused in Sarcoma
gDNA	Genomic Deoxyribonucleic Acid
GTP	Guanosine Triphosphate
H_2O	Water
H_2O_2	Hydrogen Peroxide
HD	Huntington's Disease
hSOD1	Human Superoxide Dismutase1
HSP	Hereditary Spastic Paraplegia
HR	Homologous Recombination
HTT	Huntingtin gene
IPTG	Isopropylβ-D-1-thiogalactopyranoside
jALS	Juvenile Amyotrophic Lateral Sclerosis
kb	Kilobase
kDa	Kilodalton
LB	Lysogeny Broth
LMN	Lower Motor Neuron
MBR	Metal-Binding-Region
mg	Miligram
ml	Mililiter
MN	Motor Neuron
MND	Motor Neuron Disease
mRNA	Messenger Ribonucleic Acid
mSOD1`	Mutant Superoxide Dismutase1
mtDNA	Mitochondrial Deoxyribonucleic Acid
ND	Neurodegenerative disease
NMDA	N-Methyl-D-aspartic acid
NADPH	Nicotinamide adenine dinucleotide phosphate
OPTN	Optineurin
PCR	Polymerase Chain Reaction
PD	Parkinson's Disease
p.m.	Post Meridiem

ROS	Reactive Oxygen Species
RNA	Ribonucleic Acid
RNAi	Ribonucleic Acid Interference
sALS	Sporadic Amyotrophic Lateral Sclerosis
SDS	Sodium Dedocyl Sulfate
SETX	Senataxin
SMA	Spinal Muscular Atrophy
SOD1	Superoxide Dismutase1
SPG11	Spatacsin
TARDBP	TAR DNA Binding Protein
TBE	Tris/ Borate/ Ethylenediaminetetraacetic Acid
TIM	Translocator Inner Membrane
TOM	Translocator Outer Membrane
tRNA	Transfer Ribonucleic Acid
UAS	Upstream Activating Sequence
UPR	Unfolded Protein Response
UV	Ultraviolet
VABP	Vesicle-associated Membrane Protein-associated Protein B
WTL	Wild-Type-Like
wtSOD1	Wild-Type SOD1
X-GAL	5-Bromo-4-chloro-3-indolyl β-D-galactopyranoside

LIST OF SYMBOLS

A	Alanine
°C	Centigrade Degree
C, Cys	Cysteine
CO_2	Carbon dioxide
Cu^{+2}	Cupper Ion
D	Aspartic Acid
E	Glutamic Acid
F	Phenylalanine
G	Glycine
H, His	Histidine
H_2O	Water
H_2O_2	Hydrogen Peroxide
I	Isoleucine
K	Lysine
KCl	Potassium Chloride
KOAc	Potassium Acetate
L	Leucine
LiCl	Lithium Chloride
$MgCl_2$	Magnesium Chloride
N	Asparagine
NaCl	Sodium Chloride
O_2^-	Superoxide
$PI(3,5)P_2$	Phosphatidylinositol (3,5)-bisphosphate
Q	Glutamine
R	Arginine
S	Serine
T	Threonine
V	Valine
x g	Times Gravity
Y	Threonine

1. INTRODUCTION

Neurodegenerative diseases (NDs) are complex disorders, characterized by progressive nervous system dysfunction. Alzheimer's Disease (AD), Parkinson's Disease (PD), Amyotrophic Lateral Sclerosis (ALS) and Huntington's Disease (HD) are some of the prominent examples of NDs. These diseases all have adult-onset characteristics and with the relatively extended human life span in developed countries, they affect more people each year, thus become more common (Dong *et al*., 2009).

Many NDs share similar features, such as formation of abnormal protein aggregates and progressive degeneration of specific neuronal populations (Ghosh and Feany, 2004). Despite these common characteristics, the location of neuronal loss and the abnormal protein aggregation vary depending on the type of the disease (Figure 1.1), this creates discrepancies between the sub-types of NDs (Farooqui and Farooqui, 2009).

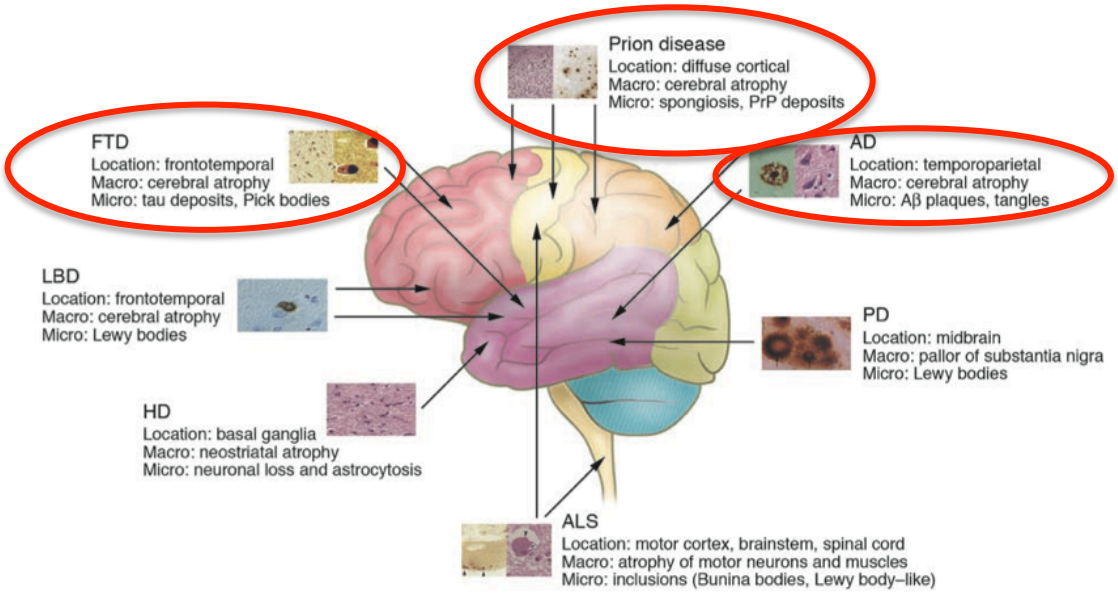

Figure 1.1. NDs and the corresponding brain regions affected (Bertram and Tanzi, 2005).

NDs are often classified according to their genetic etiology, clinical features or pathology. Regarding their genetic causes, either a single gene may be responsible for the disease development (e.g. *HTT* for Huntington Disease), or as in the case for many NDs, the causative effect may not be due to a single gene, so unknown or environmental mechanisms are thought to be involved in disease development. (e.g. ALS) (Shulman *et al.,* 2003). Regarding their clinical features NDs can be grouped as movement disorders [HD, PD and Motor Neuron Disease (MND)] and dementias [(AD and Frontotemporal Dementia (FTD)]. Additionally, NDs can be grouped according to the affected-neuron type, as dopaminergic (PD), motor (MND) and GABAergic neurons (HD) (Hirth, 2010).

Among these groups, MNDs display rapidly progressive, adult-onset characteristics (Sathasivam, 2010). ALS, Spinal Muscular Atrophy (SMA) and Hereditary Spastic Paraplegia (HSP) are some common examples of MNDs (Dion *et al.,* 2009). The pathology of the disease involves the selective degeneration of the upper and/or lower motor neurons (MNs) and due to the specific degeneration of MNs, the resulting clinical appearance of MNDs is characterized by muscle weakness and/or spastic paralysis (Hirth, 2010; Dion *et al.,* 2009) (Figure 1.2.).

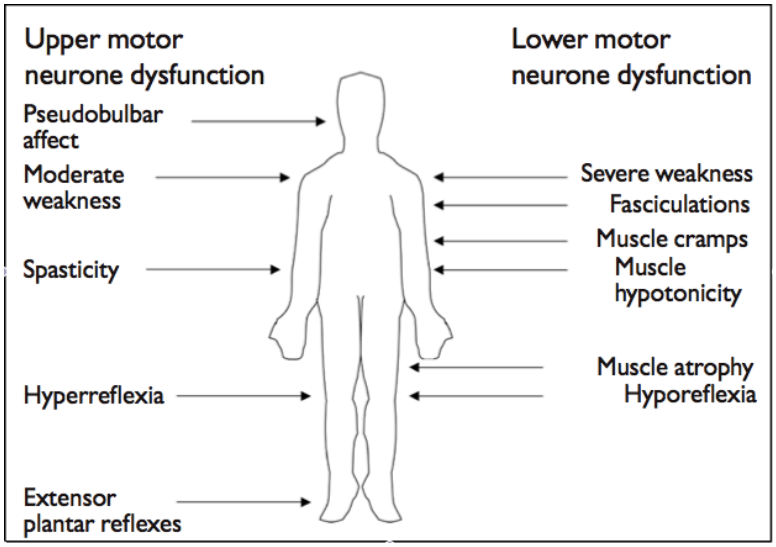

Figure 1.2. MN dysfunction in MND (Sathasivam, 2010).

1.2. ALS

ALS is the most common MND and was first described by the French neurologist Jean Martin Charcot in 1869. The characteristic feature of this adult-onset disease is the selective death of upper and lower motor neurons. Disease-mediated damage to MNs prevents neurons from stimulating the muscle eventually leading to muscle weakness and degeneration (Figure 1.3.). The degeneration of the upper motor neurons causes slow speech, spasticity and hyperreflexia; while the clinical appearance of lower motor neuron degeneration is general weakness, muscle atrophy, paralysis and fasciculation (Aguilar *et al*., 2007; Lomen-Hoerth, 2008). In general, ALS affects all muscles except the urethral sphincter and the extraocular muscle (Pasinelli and Brown, 2006).

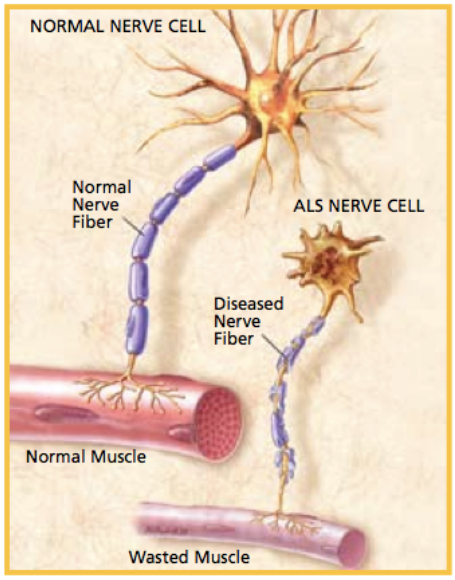

Figure 1.3. Comparison between a normal neuron and an ALS-damaged neuron (www.sfn.org/brss).

Generally, 5-10% of ALS patients have a family history (familial ALS), whereas there is no apparent genetic contribution for the remaining portion (sporadic ALS) (Bosch, 2010). Familial ALS (fALS) and sporadic ALS (sALS) patients cannot be distinguished clinically from each other, although there are some minor differences between them: compared to sALS, fALS cases are characterized by a nearly ten year earlier age of onset; fALS have obviously an equal male: female ratio; and fALS mostly shows slower progression (Ticozzi *et al.,* 2011). Juvenile ALS (jALS), which constitutes a minor portion

of ALS, affects people before the age of 25. Compared to fALS, jALS patients have prolonged survival (Sabatelli *et al.,* 2008).

ALS has a prevalence (total number of cases at a given time) of 4-6 per 100,000, and its incidence (number of new cases in a year) is 1-2 per 100,000, with a male:female ratio of 1.6:1 (Mitchell and Borasio, 2007). Moreover, ALS is usually fatal within 3-5 years following its diagnosis due to its rapidly progressive nature. (Valdmanis and Rouleau, 2008).

1.2.1. Molecular Genetics of ALS

The most common causative genetic factor in ALS is the specific effect of mutations in the gene, SOD1 and these mutations are responsible for 20% of fALS cases (Meireles and Chalabi, 2009). The vast majority of *SOD1* mutations is inherited in a dominant manner with the only exception of D90A which is known to be inherited recessively in some populations (Valentine *et al.,* 2005).

The initial finding of the ALS-related *SOD1* mutations was in 1993 (Rosen *et al.*, 1993). Almost two decades after this discovery, several other genes have been shown to be responsible for the pathology of the disease: *ALS2* (Alsin), *DCTN1* (Dynactin1), *SETX* (Senataxin), *VAPB* (VAMP-associated protein B), *ANG* (Angiogenin), *TARDBP* (TDP-43), *FUS*/*TLS* (Fused in Sarcoma), *OPTN* (Optineurin), *SPG11* (Spatacsin), *VCP* (Valosin-containing protein), *ATXN2* (Ataxin-2) (Hadano *et al.,* 2001; Chen *et al.,* 2003; Chen *et al*., 2004; Nishimura *et al.,* 2004; Chen *et al*., 2006; Sreedharan *et al.*, 2008; Sreedharan *et al.*, 2009; Maruyama *et al.*, 2010; Orlacchio *et al*., 2010; Johnson *et al.,* 2010, Elden *et al.,* 2010) (Table 1.1.). Among these genes, research on *TARDBP* and *FUS/ TLS* is promising, because of their relatively big contribution to fALS genetics (*TARDBP* 4-5%; *FUS* 5%) following SOD1 gene mutations (Kiernan *et al.,* 2011).

Table 1.1. Causative genes for ALS pathogenesis.

ALS type	Locus	Clinical Pattern	Inheritance Pattern	Gene	Protein
ALS1	21q22.1	Classical	AD	SOD1	Cu/Zn superoxide dismutase
ALS2	2q33-35	Young onset, UMN	AR	Als2	Alsin
ALS3	18q21	Classical	AD	?	?
ALS4	9q34	Young onset, slow	AD	SETX	Senataxin
ALS5	15q15-21	Young onset	AR	SPG11	Spatacsin
ALS6	16p11.2	Classical	AD	FUS	Fused in sarcoma
ALS7	20p13	Classical	AD	?	?
ALS8	20q13.33	Varied	AD	VAPB	VAMP-associated protein B
ALS9	14q11	Classical	AD	ANG	Angiogenin
ALS10	1q36	Classical	AD	TARDBP	TAR DNA-binding protein
ALS11	6q21	?	AD	FIG4	PI(3,5)P(2)5-phosphatase
ALS12	10p15-p14	Classical	AR/ AD	OPTN	Optineurin
ALS13	12q24.1	SCA2	AD	ATXN2	Ataxin-2
ALS14	9p13.3	?	AD	VCP	Valosin-containing protein
LMND	2p13	LMND	AD	DCTN1	Dynactin
ALS-FTD1	9q21-22	With FTD	AD	?	?
ALS-FTD2	9p13.2-21.3	With FTD	AD	?	?

1.2.2. Cu/ Zn Superoxide Dismutase (SOD1)

In the human genome, *SOD1* extends over a length of 9.3 kb. The gene comprises five exons encoding a 32 kDa protein of 153 highly conserved amino acids. This is the well-conserved cytoplasmic antioxidant enzyme SOD1, which is also known as Cu/Zn superoxide dismutase. *SOD1* is ubiquitously expressed within the organism and has relatively higher expression levels in nervous tissue, liver and erythrocytes. Therefore, the product of the gene, SOD1, is an abundant cellular protein representing approximately 1% of all cytoplasmic proteins.

SOD1 functions as a homodimeric enzyme and consists of two subunits. Each subunit displays an eight-stranded Greek key β-barrel fold and also contains seven β-loops (Figure 1.4.). Some portions of the β-loops are functional domains, (*e.g.* loop IV belongs

to “Zn binding loop” and loop VII belongs to “electrostatic loop”) forming the active site of the enzyme (Kato *et al.,* 2000). The Zn binding loop corresponds to the residues 63-84, while the electrostatic loop corresponds to the residues 121-144. The residues in the electrostatic loop are charged and essential for the guidance of the negatively charged substrate, O_2^-, to the active site entrance. This electrostatic guidance makes the SOD1 enzyme highly specific for its substrate (Uversky and Fink, 2007).

To function properly, each subunit of the SOD1 enzyme has to bind properly both to one copper and to one zinc ion. His46, His48, His63 and His120 are involved in copper ion binding and His63, His71, His80, Asp83 are involved in zinc ion binding. His63, the residue that is also known as imidazolate ligand, interacts with both ions. The ligand connects both metal ions to each other and also links them to one side of the β-barrel. Asp124 is another important residue that is responsible for correcting the geometry of the metal binding sites. There is also a conserved intrasubunit disulfide bond between Cys57 and Cys146 and an intersubunit disulfide bond between Cys6 and Cys 111(Valentine *et al.,* 2005).

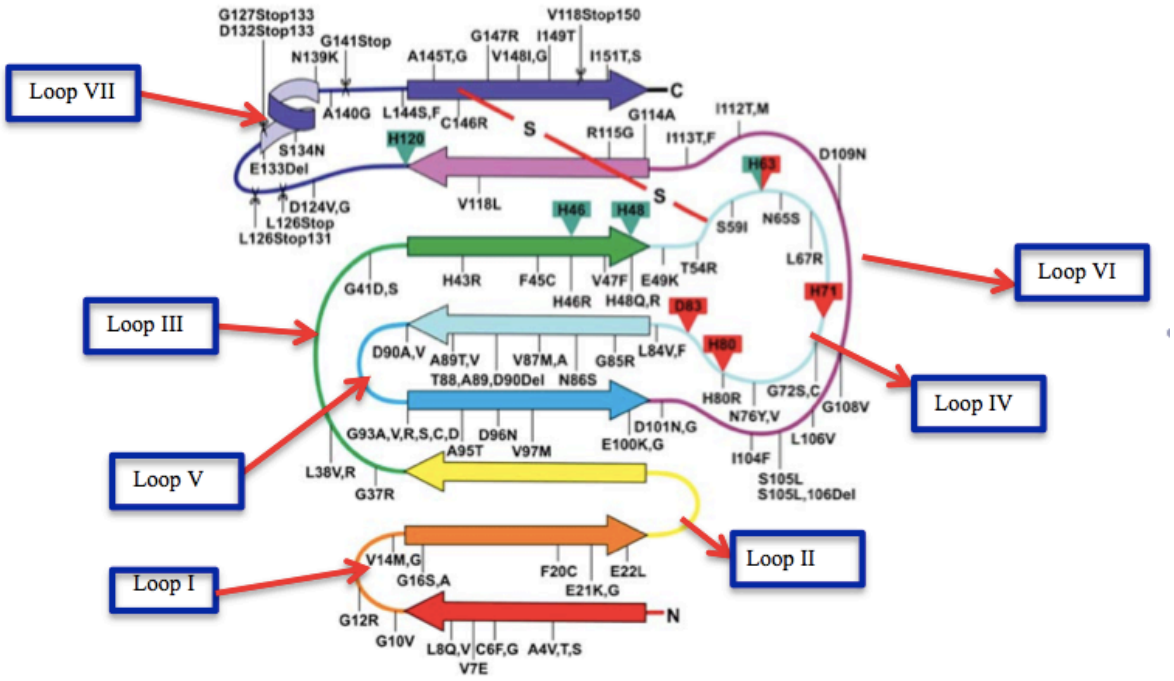

Figure 1.4. Secondary structure of SOD1 and the representation of fALS-related mutations (adapted from Valentine *et al.,* 2005).

The enzyme catalyzes conversion of superoxide radicals (O_2^-) to hydrogen peroxide (H_2O_2) and molecular oxygen (O_2) (Ticozzi *et al.,* 2011). H_2O_2 is then further detoxified to H_2O by glutatione peroxidase or catalase (Cleveland, 1999), as shown below:

$$O_2^- + \text{SOD1-Cu}^{2+} \rightarrow O_2 + \text{SOD1-Cu}^+$$
$$O_2^- + \text{SOD1-Cu}^{+} + 2H^+ \rightarrow H_2O_2 + \text{SOD1-Cu}^{2+}$$

This dismutase activity of the superoxide anion is mediated by protein-bound copper ions that alternate between reduced and oxidized forms (Uversky and Fink, 2007).

1.2.2.1. The Discovery of Mutations In The SOD1 Gene. Today, it is known that mutations in the SOD1 gene lead to ALS (ALS1); this relation was first described in 1991 as linkage to chromosome 21q22.1 (Siddique et al., 1991). Two years later, eleven disease-associated mutations were found in *SOD1* (Rosen *et al.,* 1993). To date, various studies on *SOD1* have elucidated more than 150 mutations distributed throughout the five exons of the gene (Ticozzi *et al.,* 2011). The vast majority of these mutations are missense substitutions, but at a total of eight frameshift deletions and five insertions have also been mapped to the exons 4 and 5 (Ticozzi *et al.,* 2011).

The ALS1 causing mutations in *SOD1* can be classified into two categories: Metal-binding-region (MBR) mutants and wild-type-like (WTL) mutants (Table 1.2.). This categorization considers the biochemical and biophysical properties of the SOD1 mutants. WTL mutants are located in the β-barrel or dimer interface region of the enzyme, while MBR mutants are found in the electrostatic and zinc binding loops (Valentine *et al.,* 2005; Murray, 2006).

Table 1.2. Categorization of some SOD1 mutations (Valentine *et al.,* 2005).

Wild-type-like (WTL) mutants				Metal-binding region (MBR) mutants
A4V	G72S	G93V	N139K	H46R
V7E	D76Y	E100G	L144F	H48Q
L8Q	L84V	E100K	L144S	H80R
G37R	N86S	D101N	A145T	G85R
L38V	D90A	D101G	V148G	D124V
G41D	G93A	I113T	I149T	D125H
G41S	G93R	R115G		S134N
H43R	G93C	E133Del		C146R

The WTL mutants have full SOD1 enzymatic activity and their biophysical properties are the almost same with wild-type SOD1, whereas MBR mutants have much less catalytic activity and metal binding capacity (Durer *et al*., 2009).

Apart from these discrepancies, there is no definite link between the disrupted dismutase activity and the clinical manifestation of the mutation. Indeed, even within a single mutation group (WTL or MBR), there is no genotype-phenotype correlation (Table 1.3.). For example, relative survival time for WTL mutants varies from mutation to mutation: it is more than 17 years for G37R and 1–3 years for L38V (Valentine *et al.,* 2005). Alternatively, there are some mutations which are linked to specific clinical features; *e.g*., A4V, the most common mutation in North America, always leads to a rapidly progressing disease phenotype.

Table 1.3. Phenotype variation among SOD1 mutants (Murray, 2006).

Predominant clinical feature	**SOD1 mutation**
Early onset	G37R, L38V, H46R, H80A, G85R, L106V
Late onset	I113T
Slow progression	E21G, G37R, G41D, H46R, D90A, G93A, G93V, G93C, I104F, I113T, I151T, L144S, L144F
Rapid progression	A4T, A4V, H48Q, N86S, L106V, V148G
Short survival	A4V
Long survival	G37R, G41D, H46R, G93A
Bulbar onset	A4V, L8O, D76Y, D90A, V148I, I151T
Predominant affection of the 2nd motor neuron	A4V, H80A, L84V, D101N

Table 1.3. Phenotype variation among SOD1 mutants (Murray, 2006) (continued).

Associated with dementia	D76T
Female predominance	G41D
Prolonged central motor conduction time	K12A, D76Y, D90A
Low penetrance	D90A, I113T
Hundred percent penetrance by age 70	L38V, E100G, I113T
Dominant and recessive transmission	D90A, D96N
Reduced capacity to bind copper	H46R, H48Q
Occurrence in sALS	H80A, D90A
Non-penetrance	V4G, G16S, G21L, A76T, A101A, I113T
Neurofibrillary inclusions	A4V, H48Q, I113T

SOD1 mutations are largely found in exons 4 and 5, whereas exon 3 has fewer mutations. As mentioned earlier, these mutations generally result in missense mutations, but some of them cause frameshifts, truncations, deletions, or insertions. Epidemiological studies indicate some mutations are population-specific: e.g., A4T in Japanese, D76V in Hispanic, L144F in Slavic populations.

Because SOD1 enzyme is ubiquitously expressed and has a major antioxidant role in cells, the pathologic nature of the mutation was thought to be a “loss of function”. After some results emerged in the field indicating that dismutase activity remains unchanged for many ALS-causing *SOD1* mutations, the assumptions of the effect of particular mutations have turned towards the protein’s acquisition of toxic function—thus the “loss of function” hypothesis has been replaced by the “gain of function” hypothesis.

1.2.3. Possible Mechanisms In mSOD1-linked ALS

SOD1 gene is ubiquitously expressed within the organism, but all of the SOD1 mutations give rise to a tissue specific disease—ALS. In order to explain how mutant SOD1 (mSOD1) selectively targets motor neurons in mSOD1-related ALS, at least six explanations for a gain-of-function hypothesis have been suggested: oxidative stress, intracellular protein aggregation, mitochondrial dysfunction, glutamate excitotoxicity, axonal transport impairments and neighboring cell pathologies (Rothstein, 2009).

1.2.3.1 Oxidative Stress. Superoxide anion, hydroxyl radicals, hydrogen peroxide and peroxynitrite are naturally occurring by-products of oxidative phosphorylation and referred to as reactive oxygen species (ROS). Indeed, neither superoxide anion nor hydrogen peroxide are highly toxic molecules. The underlying danger, associated with these molecules, is their ability to covert to more reactive species. Superoxide reacts with nitric oxide to produce peroxynitrite, whereas hydrogen peroxide is degradated to the highly reactive hydroxyl radical in a process that can be catalyzed by reduced metal ions (Shaw and Barber, 2010). These highly reactive hydroxyl and peroxynitrite radicals need to be detoxified to prevent damaging macromolecules (such as proteins, lipids, DNA) within the cell. Such damage can lead to a change in protein conformation, altering cellular membrane dynamics via oxidation of fatty acids and alterations in DNA/RNA species (Shaw and Barber, 2010). To prevent this stress, cells have detoxifying mechanisms against ROS. SOD1, catalase, and glutathione peroxidase can convert these highly reactive and toxic ROS into less toxic species; therefore, these enzymes are essential for the cell viability. Oxidative stress can arise if the balance between the production and detoxification of ROS elements is disrupted.

Compared to other tissues and cell types—with lower expression of antioxidant enzymes, high oxygen consumption and high lipid content—the central nervous system (CNS) is under a relatively high risk for ROS toxicity, and so are the motor neurons in this tissue (Murray, 2006). In support of this idea, numerous studies have reported the presence of oxidative damage to cellular macromolecules in tissue samples from fALS and sALS patients (Abreu *et al.,* 2010).

Because SOD1 has a key role in the reaction which converts superoxide anions into hydrogen peroxide and oxygen, the discovery of *SOD1*-mutations in ALS cases was promising. Several mechanisms have been proposed account for the relation between increased oxidative stress in ALS pathogenesis and altered SOD1 activity due to its mutations: i. mSOD1 becomes insufficient in effectively detoxifying superoxide anion; ii. mSOD1 becomes highly activated, thus excessive amounts of hydrogen peroxide can turn into reactive hydroxyl radicals that increase the oxidative stress within the cell; iii. mSOD1 has a dominant negative effect that inhibits the normal SOD1 enzyme which is expressed by the wild-type allele; iv. due to its abnormal conformation, mSOD1 reverts its normal

function by binding to hydrogen peroxide and promotes superoxide production (peroxidase activity). However, the results of several subsequent studies have complicated these premises: for example, a study utilizing one *SOD1* knock-out animal model showed that mutation-carrying animals did not develop the disease, while in another study it was shown that there was no difference in the peroxidase activity between A4V/G93A mutants and the wild type protein (Reaume *et al.,* 1996; Shaw and Barber, 2010). Hence, mechanisms of mSOD1 toxicity in disease have not been clarified. Almost every theory described here has its own antithesis, so it can be concluded that mSOD1 toxicity cannot solely be explained by oxidative stress mechanisms, but oxidative stress certainly has additive effects to the other mSOD1-associated pathologic mechanisms.

1.2.3.2 Intracellular Protein Aggregation. One of the characteristic features of NDs is the presence of protein aggregates. In SOD1-linked ALS, intracellular SOD1 aggregation is reported in many studies, although it is not known whether they have an ameliorative, neutral or toxic effect on the disease pathogenesis (Bruijn *et al.,* 1998; Ross and Poirier, 2004).

Two theories have been put forward to elucidate the aggregation mechanism. The first theory is based on the aberrant reactions in which mSOD1 takes role. According to this theory, aberrant reactions give rise to highly reactive radicals and induce oxidative stress within the cell. As a result of this oxidative stress, SOD1 itself can be damaged and dissociate into monomers which further constitute the aggregate formation (Rakhit *et al.,* 2004). The second theory supports the idea that mSOD1 is not as efficient as wtSOD1 in terms of its metal binding capacity, and the insufficient metal binding can lead to destabilization in the enzyme structure, which makes the enzyme susceptible for aggregation (Rakkhit *et al.,* 2002).

The finding of SOD1 aggregates in the ER led to the proposition for a new mechanism in which unfolded protein response (UPR) and heat shock proteins are involved in ALS etiology. When a protein is newly synthetized, it is aided by heat shock proteins to arrive at its final conformation. In the case of protein misfolding, additional heat shock proteins are activated by the UPR. If these additional heat shock proteins

cannot assist in protein refolding, then the protein is exported from the endoplasmic reticulum (ER) to the cytosol and, here, the ubiquitinated protein is degraded by the proteasome machinery. In ALS, mSOD1 has been found to accumulate in the ER and also inhibit the the TIM (the translocator inner membrane) and TOM (the translocator outer membrane) complexes which transports many other proteins from ER to cytosol. This inhibition of TOM/TIM by mSOD1 accumulation is thought to cause ER stress. Additionally, a decrease in proteasome activity has been found in mSOD1 overexpressing cells and tissues (Cheroni *et al.,* 2009). The decrease in proteasome activity may also lead to aggregation of other misfolded proteins. Thereby, a cell devoid of essential proteins, such as heat shock proteins, and this protein transport/degradation mechanism have been proposed to explain the toxicity of the aggregates. Paradoxically, the aggregates may sequester the mutant protein itself, functioning as a protective mechanism. Again, the causative nature of the aggregates is still unknown, but it is observed that aggregation formation is characteristic of most NDs (Pasinelli and Brown, 2006).

1.2.3.3. Mitochondrial Dysfunction. The mitochondrion is an essential organelle with various roles; such as ATP production, calcium buffering and cell survival. Therefore, mitochondrial dysfunction may result in motor neuron death by generating high levels of ROS, disrupting calcium homeostasis and initiating apoptosis (Shi *et al.,* 2010).

Mostly present as a cytosolic protein, SOD1 can also translocate to the nucleus, ER and mitochondria (Crapo *et al.,* 1992; Kikuchi *et al.,* 2006). In mitochondria, the SOD1 protein is found to be present in the inter-membrane space, inner membrane and matrix (Okado- Matsuma and Fridovich, 2001). Similar to wtSOD1, mSOD1 can also localize in the mitochondria. A study in 2002 has shown that mSOD1 is present in the mitochondria of spinal cord cells of mSOD1 transgenic mouse (Higgins *et al.,* 2002).

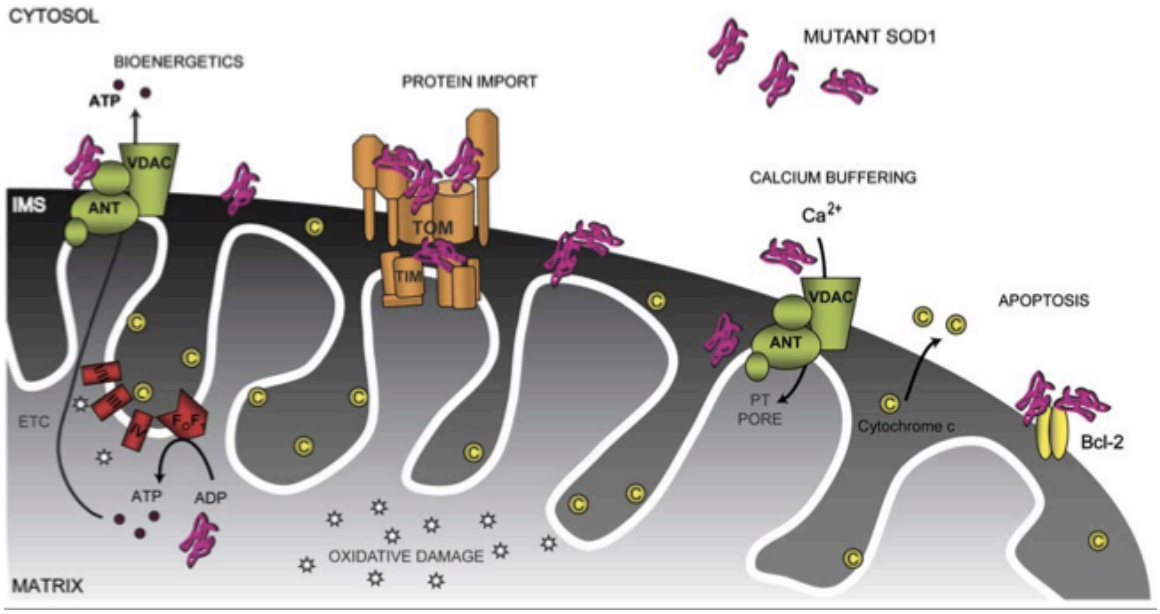

Figure 1.5. Mitochondrial dysfunction in ALS (Boillée *et al.,* 2006).

The localization of mSOD1 in mitochondria can cause damage to the organelle by several mechanisms (Figure 1.5.) (Boillée *et al.,* 2006):

- Disruption of mitochondrial morphology and bioenergetics: In the G93A SOD1 transgenic mouse, mitochondria undergo vacuolar degeneration in motor neurons. Swelling and vacuolisation of mitochondria primarily result from expansion of the intermembrane space, and is tightly linked to the accumulation of mutant SOD1 in this compartment. Also the degree of vacuolization is correlated with concentration of mutant SOD1 expressed by transgenic mice (Jaarsma *et al.,* 2001). Mutant SOD1 also causes oxidative stress that gives damage to the mitochondrial DNA (mtDNA) (Murray, 2006). MtDNA is displays a10 times higher mutation rate than genomic DNA. Part of the explanation for this is that, mtDNA lacks histones and an effective repair mechanism. These properties of mtDNA make it especially vulnerable to oxidative damage. Furthermore, mutations in mtDNA due to oxidative stress also cause mutational defects in the respiratory chain proteins (Pasinelli and Brown, 2006).
- Clogging of protein import mechanism: Mitochondria with their limited genomic DNA are not capable of producing all of the proteins required for normal function and rely on nuclear-encoded genes. Transport of nuclear-encoded products is mediated by TOM/TIM complexes. Mutant SOD1 that localizes in the

mitochondria aggregates and prevents this complex along with the mitochondrial proteome to function properly. (Boillée *et al*., 2006).

- Impaired calcium buffering: Calcium is involved in many signaling pathways that are crucial for cell survival. The mitochondrion is important for its ability to serve as a buffer for excess intracellular calcium levels in motor neurons where the expression of calcium-binding protein is relatively low. In ALS patients, as well as animal and cell culture models of ALS, there is reduction in the activity of the mitochondrial calcium buffering capacity and elevation of intracellular calcium ions (Shi et al., 2010). Furthermore, elevated calcium levels in the cytoplasm leads to glutamate-induced excitotoxicity (Tateno *et al.,* 2004).
- Apoptosis: Mutant SOD1 can also induce mitochondria-mediated apoptosis; mSOD1 has been found to interact with anti-apoptotic protein Bcl-2. One possibility is that, mSOD1 can sequester Bcl-2 into aggregates and thereby render it non-functional. Another possibility is that, upon binding to mSOD1, Bcl-2 changes its conformation and becomes toxic. Stimulation of apoptosis requires caspase activation following pro-apoptotic signals. Pro-apoptosis family member Bcl-2 translocates to the mitochondria serving as a pro-apoptotic signal and inducing the mitochondria to release cytochrome c into the cytosol which further activates the caspase cascade. The activation of this cascade eventually leads the cell to apoptosis. Although it is not certain whether motor neuron death in ALS is due to apoptosis, there are a number of studies which attempt establish connections between apoptosis and motor neuron degeneration. For example in one study, it was shown that Bcl-2 overexpression reduced neurodegeneration, delayed caspase cascade activation and prolonged survival in G93A SOD1 mice (Vukosavic *et al.,* 2000). In another study it was shown that the inhibition of caspases lead to reduced oxidative-stress-induced death in mSOD1 neuroblastoma cells (Pasinelli *et al.,* 1998).

1.2.3.4. Glutamate Excitotoxicty. Nerve impulses in motor neurons are transmitted from the presynaptic neuron to the postsynaptic neuron via glutamate, the major excitatory neurotransmitter in CNS. In order to terminate chemical neurotransmission, glutamate should be taken up from the synaptic space. Otherwise, it would continuously stimulate glutamate receptors of the postsynaptic neuron and promote calcium and sodium influx. Such a phenomenon is called excitotoxicity and can cause neuronal injury and death (Shaw and Barber, 2010) (Figure 1.6.).

Motor neurons are especially vulnerable to excitotoxicity, more than any other neuron type, mainly because they express a different type of glutamate receptor. Motor neurons express AMPA/kainate receptors for glutamate, whereas in most neurons glutamate toxicity is mediated by NMDA receptors. AMPA receptor consists of four subunits and incorporation of the subunit GluR2 into heteroretramers decreases calcium permeability. Because the expression level of this subunit is low in motor neurons, the motor neuronal AMPA/kainate receptors are more calcium permeable and therefore confer vulnerability to excessive glutamate stimulation—an observation that is supported by several studies. For example; in a study, deletion of the GluR2 gene has accelerated motor neuron degeneration (Van Damme *et al.,* 2005) and in another study, it has been reported that overexpression of *GluR2* causes reduction in the calcium permeability and increases the life span of the mSOD1 mouse model (Tateno *et al*., 2004). Motor neurons with their calcium permeable glutamate receptors and low expression levels of calcium binding proteins need to handle the excess amount of calcium, but compared to other neuronal types, motor neurons have a lower capacity to buffer calcium. Mitochondria appear as a solution for this buffering issue; but as mentioned earlier, mitochondria lose their buffering ability in the course of disease progression.

Another important issue with the glutamate excitotoxicity is the clearance of glutamate within the synaptic space. For that purpose, excitatory amino acid transporters (EAAT) are present at most synapses in CNS. During neurotransmission, EAAT2 (also known as GLT1) transports glutamate from the synaptic space into astrocytes upon glutamate release. Recent studies on the rodent models of mSOD1 showed reduction in the expression and activity of EAAT2 in the cortex as well as the spinal cord. This reduction

has been related to oxidative damage created by mSOD1 (Trotti *et al.,* 1999; Howland *et al.,* 2002).

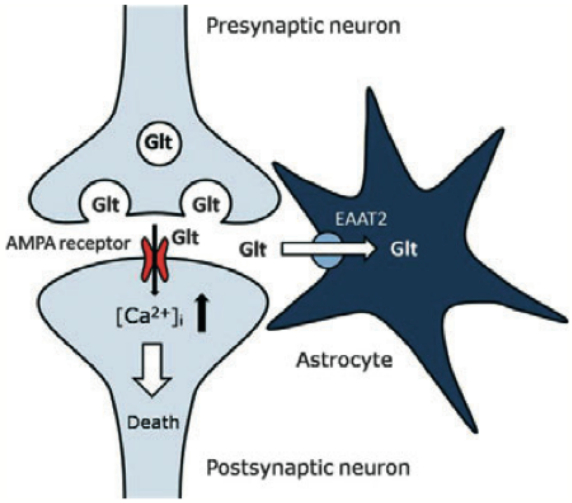

Figure 1.6. Glutamate excitotoxicity and neuronal death (Bento-Abreu *et al.,* 2010).

1.2.3.5 Axonal Transport Impairments. Neurons have a specialized cell shape. In humans, neurons typically have a cell body measuring ~6-120 μm in diameter and their axons can be a meter or more in length (Roy *et al.,* 2005). Despite their enormous length, axons lack a mechanism to ensure biosynthesis of proteins and other molecules fully autonomously. Therefore, there is a necessity for molecules originally synthesized in the cell body to be transported via a mechanism, called anterograde transport. Similarly, some information traffic occurs between synapses and the cell body by retrograde transport. The transportation of proteins is known as slow axonal transport, whereas vesicle transportation is known as fast axonal transport (De Vos *et al.,* 2008).

In transgenic G93A and G37R mice, both slow and fast anterograde transport decrease prior to disease onset, and they worsen with disease progression (Zhang *et al.,* 1997; Williamson and Cleveland, 1999). Likewise, retrograde transport is also disrupted in ALS mice (Murakami *et al.,* 2001). Mutant SOD1 impairs axonal transport in different ways: through damage to the mitochondria and reduction of ATP supply to molecular motors; pathogenic signaling can alter phosphorylation of molecular motors and cause alteration in the phosphorylation of cargoes, such as the disruption of neurofilament association with the motor proteins (De Vos *et al.,* 2008). Beside the disruptions in the antero- and retrograde transport, neurofilament accumulation in the cell body is another

prominent feature of ALS. Furthermore, there are studies with transgenic animals where motor neuron dysfunction is observed both for mice carrying a point mutation in the neurofilament subunit and for mice overexpressing these subunits (Xu *et al.,* 1993; Lee *et al.,* 1994).

1.2.3.6 Neighboring Cell Pathologies. In early studies, some types of non-neuronal cells, such as microglia and astrocytes, were found to be activated in ALS (Hall *et al.,* 1998). Subsequently, targeted expression of mSOD1 within either motor neurons, or astrocytes and microglia insufficient to cause motor neuron degeneration (Gong *et al.,* 2000; Pramatarova *et al.,* 2001). Interestingly, another study showed that when mSOD1-expressing motor neurons were surrounded by healthy neighbors, they survived longer; whereas wild-type motor neurons were damaged by their mSOD1-expressing neighbors (Clement *et al.,* 2003). Thus, from these studies, it was concluded that astrocytes and microglia also contribute to the vulnerability of motor neurons to mSOD1-mediated toxicity in an as yet unknown fashion (Figure 1.7.).

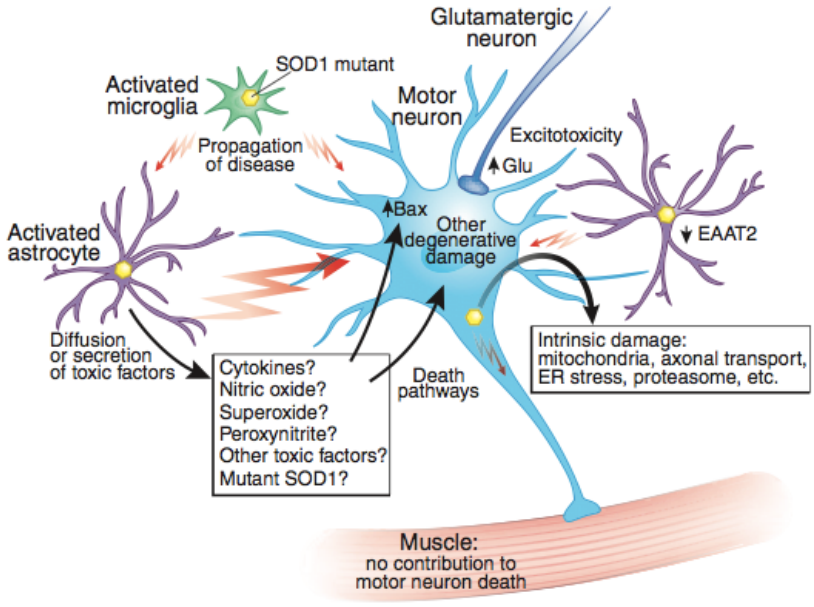

Figure 1.7. Non–cell autonomous toxicity of mutant SOD1 (Julien, 2007).

It is possible that astrocytes may be involved in disease pathology by either releasing factors that are toxic to MNs or providing neurons with inadequate trophic factors. As mentioned earlier, reduced expression and activation of EAAT2 in the astrocytes may trigger excitotoxicity and cell death (Bento-Abreu *et al.,* 2010).

Microglia are a source of NADPH oxidase, and this enzyme produces ROS during inflammation. Therefore, involvement of microglia in ALS pathogenesis may be explained with the possible induction of ROS-mediated oxidative damage to motor neurons by NADPH oxidase. In a supporting study, NADPH oxidase was up-regulated in fALS and sALS patients as well as in mSOD1 mice, and inactivation of NADPH oxidase delayed neurodegeneration and extended the survival time (Wu *et al.,* 2006).

1.2.4. *FUS/ TLS, TARDBP* and Other Genes In ALS Pathogenesis

FUS mutations account for ~5 % of fALS cases. FUS is involved in transcriptional regulation, pre-mRNA splicing and export of fully processed mRNA to the cytoplasm. FUS mutations are associated with ALS6 and to date, more than 30 mutations have been found in the gene which give rise to ALS. Although FUS is a nuclear protein, studies on tissues from FUS-linked ALS patients showed FUS localization within the cytoplasmic inclusions (Kwiatkowski et al., 2009; Vance et al., 2009). Thus, cytoplasmic inclusion formation has been hypothesized as the mechanism by which FUS mutations are involved in ALS6 development (Bento-Abreu *et al.,* 2010; Ticozzi *et al.,* 2011).

TDP-43 is encoded by *TARDBP* locus. The TARDBP protein mainly localizes primarily to the nucleus and functions in transcription and splicing regulation, microRNA processing, apoptosis, cell division, and stabilization of mRNA. Mutations in the *TARDBP* are associated with ALS10. Similar to FUS mutations, mutations in *TARDBP* are associated with inclusion formation in the cytoplasm of the neurons and glia of the primary motor cortex, brainstem motor nuclei and spinal cord. This cytoplasmic accumulation potentially results in the depletion of the protein from the nucleus, thereby disrupting pathways similar to those affected by FUS mutation. In addition, inclusions themselves may cause toxicity. Indeed, there appears to be a correlation between the degree of inclusion formation and the toxicity as a result of sequestration of essential mRNA

transcripts, abnormal cytoplasmic-nuclear RNA transport, or local translation of mRNA (Barmada *et al.,* 2010).

Als2 codes for the Alsin protein and mutations in this gene are involved in ALS2, a juvenile-onset, autosomal recessive and rare disease. Alsin acts as a guanine nucleotide exchange factor for Rab5 and other small GTPases and thought to be involved in vesicular trafficking, cytoskeletal organization and endosomal dynamics (Ticozzi *et al.,* 2011).

ALS4 is associated with mutations in the SETX gene which encodes Senataxin. This type of ALS is a juvenile-onset, autosomal recessive and rare disease with slow progression. The protein is a widely expressed DNA/ RNA helicase that is involved in repairing double-stranded DNA breaks due to oxidative damage (Suraweera *et al.,* 2007).

ALS5 is also a juvenile-onset, autosomal recessive disease. *SPG11* mutations are associated with disease progression in ALS5. The gene encodes for Spatacsin which is ubiquitously expressed in the nervous system, particularly in the cerebellum, cerebral cortex and hippocampus. The mutations in *SPG11* are also associated with HSP (Salinas *et al.,* 2008).

Mutations in vesicle-associated membrane protein-associated protein B (*VAPB*) are associated with ALS8, an adult-onset, slowly progressing disease. VAPB has a key role in unfolded protein response and when it is mutated, it may not fulfill its function and may confer vulnerablity to unfolded protein-mediated ER stress (Suziki *et al.,* 2009). VAPB is also thought to function in vesicle trafficking within the cell, because the protein localizes in ER and associates with the microtubules (Nishimura *et al.,* 2004).

ANG mutations are associated with ALS9. Angiogenin is expressed mainly in hepatocytes and secreted into the serum and the extracellular matrix. The protein stimulates tRNA transcription, ribosome biogenesis, protein translation, and cell proliferation (Smith and Raines, 2006). In ALS patients ANG mutations lead to reduced angiogenic activity of ANG in endothelial cells, and impairment of neurite extension and survival in motor neurons (Fernández-Santiago *et al.,* 2009).

The FIG4 gene encodes a phosphoinositide-5-phosphatase which is involved in autophagy by regulating $PI(3,5)P_2$ levels (Bento-Abreu *et al.,* 2010). Heterozygous loss-of-function mutations in FIG4 are found in 2% of sporadic and familial ALS patients (Chow et al., 2009). Interestingly FIG4 gene mutations are also responsible for a neurological disorder, CMT4J, a severe form of Charcot-Marie-Tooth disease (CMT) with early onset and involvement of both sensory and motor neurons (Chow *et al.,* 2009).

OPTN is a recently discovered gene that is also responsible for ALS pathogenesis. It is associated with ALS12 type of ALS. Mutations of OPTN abolish the inhibition of activation of NFκB and change the cytoplasmic distribution of optineurin (Maruyama *et al.,* 2010).

VCP gene mutations arefound to be associated with ALS pathology. VCP (valosin-containing protein) is a highly conserved AAA+-ATPase and has cellular functions including protein homeostasis through the ubiquitin proteasome system and autophagy pathways. In ALS pathogenesis it was found that, VCP mutations cause the mislocalization of TDP-43 within motor neurons in the spinal cord (Johnson *et al.,* 2010). Additionally, VCP was shown to be colocalize with an ubiquitin ligase, Dorfin, in ubiquitinated inclusions from effected neurons in ALS and PD patients (Ishigaki *et al.,* 2004).

1.2.5. Animal Models of ALS

Upon finding of the link between SOD1 mutations and ALS, researchers have begun to generate animal models based on different mSOD1 alleles to gain insights into the underlying mechanisms in ALS pathology. Eventually, much of our understanding regarding disease progression comes from these model animal studies on ALS.

1.2.5.1. Rodent Models. Following the discovery of mutations in *SOD1*, transgenic mouse models of various *SOD1* mutations have begun to emerge. The first one was a mouse model overexpressing the mutant version of human *SOD1* (*hSOD1*). The mutation of interest in the study was G93A and the mice exhibited progressive hind limb weakness which then further lead to paralysis and death (Gurney *et al*., 1994). Apart from this G93A

mutant mouse overexpression model, G37R and G85R mutant models also were generated. Studies making use of these mutant mice showed that the phenotype displayed by mutant mice was directly proportional to the amount of mutant protein generated in the tissue. Thus, this finding confirmed the nature of the SOD1 mutations as gain-of-function mutations. Following this result, mouse models were being widely used to achieve a better understanding of the toxic mechanisms mediated by mutant SOD1.

One important study, where G93A SOD1 transgenic mice were mated with copper chaperone for superoxide dismutase (CCS) knockout mice, revealed that impaired enzymatic function of SOD1 does not affect mSOD1-mediated toxicity. Although CCS is involved in copper loading to SOD1, and copper is an essential cofactor of SOD1 (Section 1.2.2.), the SOD1-mutant mouse model that lacks CCS did not show any difference in progression of motor neuron disease and the time of disease onset (Subramaniam *et al.,* 2002).

The importance of the interaction between motor neurons and their neighbors in the coarse of disease pathogenesis is well known. This finding has also arisen from the mouse model studies. In one of these studies, mSOD1 expression was restricted only to motor neurons, while in the other study it was restricted only to glial cells (Gong *et al.,* 2000; Pramatarova *et al.,* 2001). Neither of the studies resulted in motor neuron disease phenotype, indicating that an interplay between different cell types is needed to induce motor neuron death.

Mouse models are not only used for establishing an understanding of disease pathogenesis, but they are also used for testing the efficiency and reliability of the emerging therapeutic strategies. However, these trials are not always consistent with clinical studies, and as such was the case with the drug minocycline. Despite the protective effect of minocycline on mouse models, human trials have shown this treatment to be harmful in cases of human ALS (Gordon et al., 2007).

Rat models of mSOD1 have also been generated. Similar to the results of mouse models, rat models developed age-dependent degeneration of motor neurons leading to paralysis and death (Howland *et al.,* 2001; Howland *et al.,* 2002). By means of their larger

body size compared to mice, rat models have their own advantages, such as being more suitable for pharmacological manipulations.

1.2.5.2. Worm Models. C. *elegans* has also been used as an ALS model. In one of the studies, mutant *hSOD1* expression was restricted to neurons of C. *elegans* and eventually the worms were paralyzed and also exhibited protein aggregation in their neurons. In contrast, *wt hSOD1* expressing worms exhibited normal movement and no protein aggregation (Wang *et al.,* 2009). In another study, researchers generated different worm lines expressing *mSOD1* (G85R) as either homodimers or heterodimers (with wtSOD1) and to compare, they also generated lines expressing wtSOD1 as homodimers. Because G85R mutant is located in the MBR of SOD1 (Table 1.2.), the mSOD1 homodimer-expressing worm did not exhibit any dismutase activity. Large aggregate formation was observed in motor neurons in the mSOD1 homodimer-expressing worm, while there was no aggregate formation in wtSOD1 expressing worm. In addition to differences in the tendency to form aggregates, mSOD1 heterodimer-expressing worms exhibited impairment in movement, where wtSOD1-expressing worms did not (Witan *et al.,* 2008).

1.2.5.3. Fish Models. In a study from 2007, four different zebrafish lines were generated. Three of them were expressing human mutations G37R, G93A, A4V and the remaining expressed wt hSOD1. When the mutated alleles were overexpressed, an immediate axonopathy was observed in the zebrafish embryo. Again, there was no phenotypic effect for the wtSOD1 expression. The toxic effect of mSOD1 on axonal outgrowth was reported to be specific and dose-dependent (Lemmens *et.al,* 2007).

1.2.5.4. Fly Models And Why? Fruit flies are a ideal system for studying human biology. Bioinformatics analyses in the post-genomic era revealed a high degree of conservation between these two species. This conservation includes many genes and signaling pathways as well as fundamental biological pathways such as; regulation of gene expression, subcellular trafficking, synaptic transmission, synaptogenesis, and cell death. It has been shown that 75% of human disease-linked loci have homologues in *Drosophila* (Reiter *et al.,* 2001).

As a model organism, fruit flies have numerous advantages over less complex (nematode) or more expensive (mouse) models. First, they posses short reproductive and developmental cycles (10–14 days from embryo to reproductively mature adults). This feature enables screening numerous progenies in short times compared to other model organisms such as mouse models). Furthermore, maintenance of fly stocks is simple and cheap; hundreds of fly lines can be housed a small space (Ambegaokar *et al*., 2010; Cauchi and Heuvel, 2006). Also they are more amenable to genetic manipulations than mammals. A comprehensive range of approaches can be utilized for making sophisticated genetic manipulations to study gene functions (Figure 1.8.) (Chan and Bonini, 2000

Flies have simpler chromosomal genetics with only 4 pairs of homologous chromosomes, as compared to 23 in humans; 12,000 genes as compared to 20,000 in humans and simpler nervous systems ~200,000 neurons compared to ~100 billion neurons in humans. But they still display complex behaviors, such as learning and memory and perform complex motor behaviors, such as walking, climbing, courtship and flying. Therefore, fruit flies stand out as an attractive model organism for studying NDs.

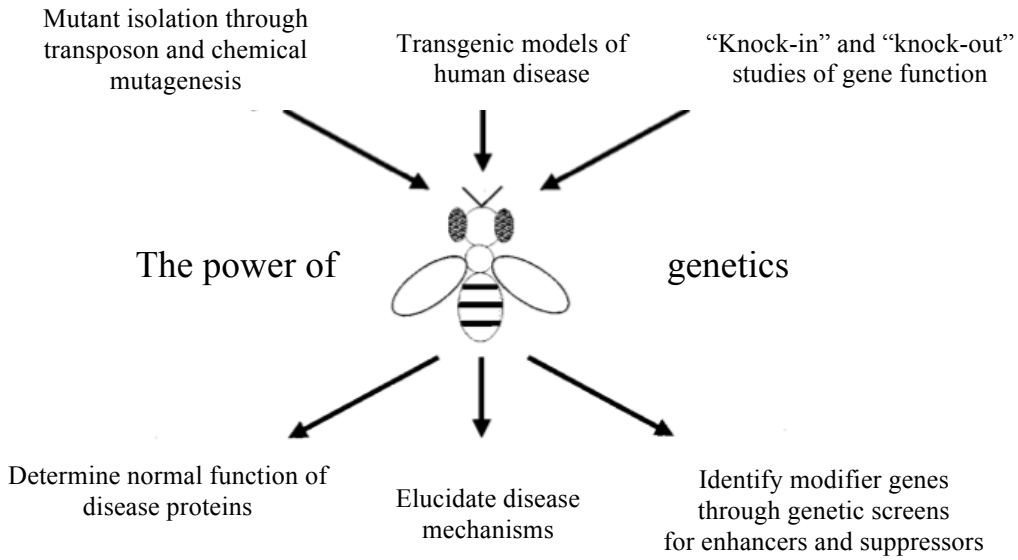

Figure 1.8. Approaches to address gene function in *Drosophila* (Chan and Bonini, 2000).

The first neurodegenerative models were successfully created in Drosophila by using human transgenes in polyglutamine disorders (Ambegaokar *et al*., 2010). For ALS research, initial studies with *Drosophila* aimed to solve the relation between mSOD1-mediated oxidative damage and life span of the flies. For this purpose, an early study used overexpression of wild type *hSOD1* specifically in motor neurons in flies. This experimental strategy resulted in an almost 40% increase in lifespan (Parkes *et al.,* 1998). The same group further investigated the effect of overexpressing fALS-associated SOD1 mutations, again specifically in motor neurons. In contrast to the results of the same experimental procedure in mice models, overexpression of fALS-related mutations did not promote paralysis and premature death in the flies. Surprisingly, the expression of mutant alleles of *hSOD1* extended lifespan, enhanced resistance to oxidative stress and partially rescued *SOD*-null mutants (Elia *et al.,* 1999). In another study, expression of wild type *hSOD1* and mutant *hSOD1* in *SOD*-null background were conducted. Expression of wild type *hSOD1* at very low levels was sufficient to rescue the life span reduction, increased oxidative stress, and impaired physiological function associated with *Sod*-null background. The introduction of human fALS *SOD1* alleles partially reversed these effects (Mockett *et al.,* 2003).

In a more recent study, selective expression of *Drosophila* SOD (*dSOD*), wild type *hSOD1*, and two mutant forms (A4V and G85R) of *hSOD1* was restricted to motor neurons. Initially, climbing properties of the flies expressing the wild type and mutant forms of the *hSOD1* seemed similar to dSOD expressing flies. After a certain time, *hSOD1* expressing flies (both wt and mutated forms), but not the dSOD expressing ones, exhibited progressive climbing defects. An interesting finding was that loss of climbing was not observed only for flies expressing mutant forms of hSOD1, but also for the flies expressing human wtSOD1. Although *hSOD1* and *dSOD* are highly similar, *hSOD1* may be recognized as a toxic mutant form of *SOD* in *Drosophila*. Additionally, accumulation of *hSOD1* in motor neurons was observed in an age-dependent manner (Watson *et al.,* 2008).

1.3. Why Homologous Recombination?

The fundamental aims in the study of neurodegenerative diseases with animal models are to elucidate underlying pathogenic pathways and eventually develop effective treatments for the diseases (Section 1.2.5.). According to the nature of mutations, different methods may be necessary for understanding the pathology of the disease: For example, overexpression studies for gain-of-function mutations, RNAi-mediated knockdown for loss-of-function and gene targeting for either type of mutations.

Gene targeting takes the advantage of homologous recombination (HR) to modify an endogenous gene sequence with an introduced DNA fragment. Initial studies with multicellular organisms were established in mouse embryonic stem cells (Capecchi, 1989) and substantially applied in human somatic cells (Hanson and Sedivy, 1995). Gene targeting is used for observing the phenotypic consequences of specific gene mutations in disease pathology.

Previous studies in *Drosophila* have utilized the Gal4/ UAS binary system for generating human disease models. Gal4 is a yeast activator and binds to upstream-activating sequence (UAS). In this system, expression of Gal4 is mediated by a strong and tissue-specific promoter. The counterpart, UAS is placed near a gene of interest. These two different transgenes are injected into flies. Animals expressing Gal4 and containing UAS linked to and the gene of interest construct are crossed with each other and finally targeted overexpression is achieved. However, with this method additional and undesired phenotypic outcomes can be observed due to overexpression of the gene and the fact that promoter is not the natural promoter of the gene of interest. This makes Gal4/ UAS system less powerful and less reliable than HR.

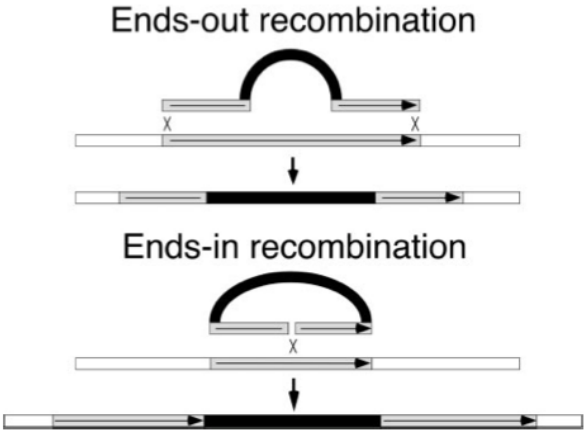

Figure 1.9. Two different vector designs in HR (Gong and Golic, 2003).

In *Drosophila,* HR-based gene targeting was developed in the beginning of 2000s. (Rong and Golic, 2000; Rong and Golic, 2001; Rong *et al*., 2002; Gong and Golic, 2003). HR can be achieved by two strategies; "ends-in" or "ends-out". These two approaches use differently arranged donor DNA constructs (Figure 1.9.). In the case of "ends-in targeting" method, DNA double-strand break (DSB) is made in the donor DNA fragment within a stretch of DNA that is homologous to the target locus, and it results in the insertion of the donor, generating a duplication of the targeted region. In "ends-out targeting", DSBs are provided at each end of a homologous segment and causes a segment of chromosome to be replaced with an introduced segment (Yu and Jiao, 2010).

HR can be used for introducing disease-causing human mutations into endogenous *Drosophila* genes. Because endogenous gene regulation remains intact by this method, mutations introduced into endogenous *Drosophila* genes may provide accurate genetic models of disease (to be discussed in more detail in Section 4).

2. PURPOSE

ALS is the most common motor neuron disease, it is very progressive being fatal within three to five years after diagnosis. The dichotomy present in almost all neurodegenerative diseases applies also to ALS: most patients are isolated incidences (sporadic ALS), whereas 10% of the patients are familial (fALS). Since the pathology of sALS and fALS are almost indistinguishable, the mutations giving rise to the pure genetic form of the disease are expected to give insights into disease mechanisms. Therefore designing animal models for functional studies is a major way of understanding the molecular mechanism underlying ALS.

The aim of this thesis is to establish the methodology of homologous recombination using *Drosophila* as a model system at NDAL laboratory in a structured collaboration with Robert Reenan laboratory at Brown University. The specific aim of this study is to introduce two different ALS-linked human SOD1-mutations (G37R and H48R) into *Drosophila* dSOD gene. Both, G37R and H48R have conserved amino acids at positions 37 and 48, respectively, among many different species; in addition, these two mutations are phenotypically different from each other in the respect that G37R is a wild-type-like mutation, while H48R is a metal-binding-region-specific lesion.

3. MATERIALS

3.1. Fly Stocks

Fly stocks were obtained from the Bloomington Stock Center (www.flystocks.bio.indiana.edu).

Table 3.1. Fly Stocks.

Genotype and Stock Description	Stock Number
w^{1118}	BSC 3605
y w Cre; noc^{Sco}/CyO y^1 w^{67c23} P{$y^{+mDint2}$=Crey}1b; noc^{Sco}/CyO	BSC 766
y w ey-FLP $y^{d2}w^{1118}$ P{$ry^{+t7.2}$=ey-FLP.N}2	BSC 5580
y w;FLP-I-SceI noc^{Sco}/CyO y^1 w*; P{ $ry^{+t7.2}$=70FLP}11 P{ $v^{+t1.8}$=70I -SceI}2B noc^{Sco}/CyO, S^2	BSC 6934

3.2. Maintenance of Flies

Table 3.2. Fly maintenance materials.

Fly Food Mix	Fisher Scientific, USA
Fly Morgue	70% Ethanol

3.3. Buffers and Solutions

3.3.1. DNA Isolation

Table 3.3. DNA isolation materials.

Chloroform, extra pure	Merck, Germany
Ethanol, 70%	Sigma, USA
Isopropanol, extra pure	Merck, Germany
5M KOAc- 6M LiCl mix (1/ 2.5)	LiCl, Merck, Germany KOAc, Sigma, USA
Phenol:chloroform:isoamyl alcohol	25: 24: 1
RNase A	20 µg/ml
Solution A	100 mM Tris (ph 7.5) 100 mM EDTA 100 mM NaCl 0.5% SDS

3.3.2. Cloning

Table 3.4. Cloning materials.

10X Bovine serum albumin (BSA)	New England Biolabs, USA
10X T4 Ligase Buffer	New England Biolabs, USA
Ampicillin	Sigma, USA
Calf Intestine Phosphatase (CIP)	New England Biolabs, USA
E.*coli* strain	XL1-Blue competent cells, Stratagene
Isopropylβ-D-1-thiogalactopyranoside (IPTG) 5-Bromo-4-chloro-3-indolyl β-D-galactopyranoside (X-GAL) solution	32 mg/ml IPTG and 40mg/ml X-GAL; Bioline USA Inc.
Kanamycin	Sigma, USA
LB agar	1Lt LB medium + 20g Agar

Table 3.4. Cloning materials (continued).

LB medium (1Lt)	10 g Tryptone 5 g NaCl 5 g Yeast extract
T4 Ligase	New England Biolabs, USA

Table 3.5 Restriction enzymes and corresponding buffers.

*Acc*65I [5' G/TACC 3']	10X Buffer 3, New England Biolabs, USA
*Asc*I [5' GG/ CGCGCC 3']	10X Multi core buffer, New England Biolabs, USA
*Bsi*WI [5' C/GTACG 3']	10X Multi core buffer, New England Biolabs, USA
*Eco*RI [5' G/AATTC 3']	10X NEBuffer *Eco*RI, New England Biolabs, USA
*I-Sce*I [5'AGTTACGCTAGGGATAA/CAGGGTAATATAG 3']	10X NEBuffer *I-Sce*I (10X), New England Biolabs, USA
*Not*I [5' GC/GGCCGC 3']	10X Buffer 3, New England Biolabs, USA

3.3.3. Gel Electrophoresis

Table 3.6. Gel electrophoresis materials.

0.5X TBE buffer (pH 8.3)	0.89 M Tris-Base 0.89 M Boric Acid 20 mM Na_2 EDTA

Table 3.6. Gel electrophoresis materials (continued).

6X DNA Loading Dye	10 mM Tris-HCl (pH 7.6) 0.03% Bromophenol Blue 0.03% Xylene Cyanol FF 60% Glycerol 60 mM EDTA
Agarose	Prona, Poland
DNA ladder, 1kb	New England Biolabs, USA Fermentas, Lithuania
Ethidium Bromide (EtBr)	10 mg/ml

3.3.4 Polymerase Chain Reaction

3.3.4.1. PCR of Homolog Arms

Table 3.7. Materials for homolog arm PCR.

10 mM dNTP	New England Biolabs, USA
5X Phusion HF Reaction Buffer	New England Biolabs, USA
Phusion High-Fidelity *Taq* Polymerase (2000 units/ml)	New England Biolabs, USA

3.3.4.2. pre-Cre PCR

Table 3.8. Materials for pre-Cre PCR.

10X *Taq* Buffer with KCl	Fermentas, Lithuania
2 mM dNTP	Fermentas, Lithuania
25 mM $MgCl_2$	Fermentas, Lithuania
Taq Polymerase (5 units/µl)	Fermentas, Lithuania

3.3.4.3. post-Cre PCR

Table 3.9. Materials for post-Cre PCR.

10 mM dNTP	Fermentas, Lithuania
10X High Fidelity PCR buffer with 15mM $MgCl_2$	Fermentas, Lithuania
High-Fidelity *Taq* Polymerase (5units/µl)	Fermentas, Lithuania

3.3.5. Sequencing

- Agencourt Clean Seq, Beckman Coulter Genomics, USA

3.4. Kits

- Maxwell 16 Tissue DNA kit, Promega, USA
- Wizard® SV Gel and PCR Clean-Up System, Promega, USA
- Zero Blunt® TOPO® PCR Cloning Kit, Invitrogen, USA
- PureYield™ Plasmid Miniprep System, Promega, USA
- BigDye® Terminator v3.1 Cycle Sequencing Kit, Applied Biosystems, USA
- QuickChange XL Site-Directed Mutagenesis Kit, Stratagene, USA
- QIAquick Gel Extraction Kit, Qiagen, USA

3.5. Fine Chemicals

3.5.1. Vectors

3.5.1.1. Cloning Vector

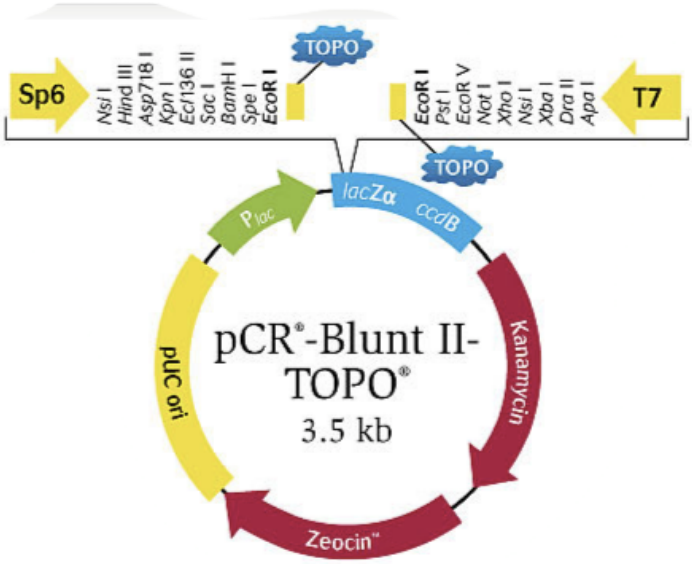

Figure 3.1. Map of the pCR –Blunt II- TOPO Vector (www.invitrogen.com).

3.5.1.2. Targeting Vector:

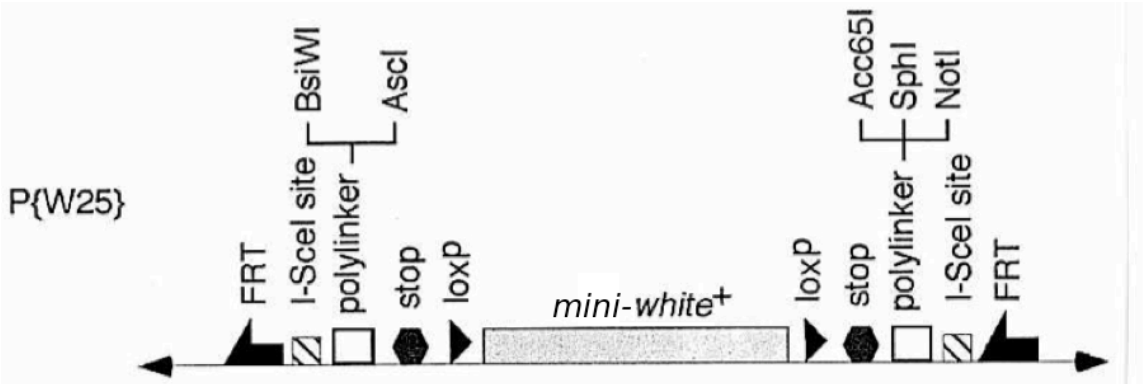

Figure 3.2. Map of the P[w25.2] targeting vector- 8968kb (https://dgrc.cgb.indiana.edu).

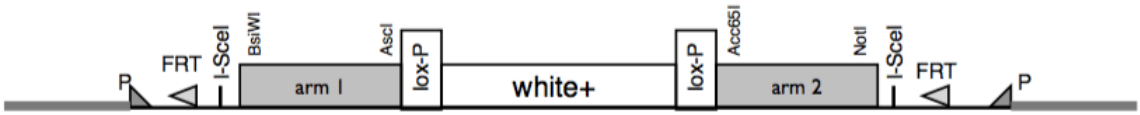

Figure 3.3. p-elements, FRT sites, I-*Sce*I recognition sites, mini-white gene, loxP sites and homology arms (Staber *et al*., 2011).

3.5.2. Primers

Table 3.10. Primer sequences for homolog arm PCR.

Arm1	**F:** 5' TCGTACGCATGTGGAAGGAAGCGCAGCGAGCGGCG 3'
	R: 5' TGGCGCGCCTCGGCACTGAAACATAACCTGTAATCATC 3'
Arm2	**F:** 5' TGGTACCGCTGCCTATAAATATTTCCGTTTAACGTGTGTC 3'
	R: 5' TGCGGCCGCGCGAGGAGTCCATCGGCGAGAGGTCGATGG 3'

Table 3.11. Site-directed mutagenesis primers.

G37R	**F:** 5'GTGAAGGTCTCCGGTGAGGTGTGCCGCCTGGCCAAGGGTCTGCACGG3'
	R: 5'CCGTGCAGACCCTTGGCCAGGCGGCACACCTCACCGGAGACCTTCAC3'
H48R	**F:** 5'GGGTCTGCACGGATTCCACGTGCGCGAGTTCGGTGACAACACCAATG3'
	R: 5'CATTGGTGTTGTCACCGAACTCGCGCACGTGGAATCCGTGCAGACCC3'

Table 3.12. Sequencing Primers for Arm1 and Arm2.

Seq 3.5	5' CGTGTGTCTATTAACAAATG 3'
Seq1	5' GGGCAAATAGTGAGGCCCATGGGTG 3'
Seq1R	5' GCTCTTCGCGTGCGTTCATGTTCC 3'
Seq2	5' GTAACAAGCAAGCAAACCACACAAGTAAC 3'
Seq3	5' GAATAGTTCCCGCCACTGTCATTGG 3'
Seq4	5' GATCTTGGCCAGGGTGGACACGAGCTG 3'
Seq5	5' GTAAATCAAGATACTCGCCACATGAGTAG 3'

Table 3.12. Sequencing Primers for Arm1 and Arm2 (continued).

Seq6	5' GTGTGAGATAAAGGCATAGGATCAGTGGG 3'
Sp6	5' ATTTAGGTGACACTATAG 3'
T7	5' TAATACGACTCACTATAGGG 3'

Table 3.13. Primer sequences for junction sequencing PCR.

Arm1	**pW25Fa:** 5' GTGCAGGCACAGTGGGACAAAGTG 3'
	pW25R: 5' CCATGCCGTAGACGCAACTCAGCGG 3'
Arm2	**pW25Ra:** 5' GCAACGAAGCTCTCTCGCGCGGAGC 3'
	Seq7: 5' CCTGCTCGGTGAGGAACTTGGAAACG 3'

Table 3.14. Primer sequences for pre-Cre PCR.

Arm2	**SODVR2:** 5'CCTGAAGCTGCTGTCCTCGCTTACGGTGC3'
	ACC2: 5'GACGCTCCGTCGACGAAGCGCCTC3'

3.6. Equipment

Table 3.15. Equipment used in this thesis.

Equipment	**Model**
Balance	TE612, Sartorius, Germany
Centrifuge	Centrifuge 2-16K, Sigma, USA
CO_2 Tank	Genç Karbon, Turkey
Deep Freezer	2021D (-20 °C), Arçelik, Turkey
DNA extraction	Maxwell® 16 System, Promega, USA

Table 3.15. Equipment used in this thesis (continued).

Documentation System	GelDoc Documentation System, BIO-RAD, USA
Electrophoretic Equipment	EC250-90 Compact Power Supply, Thermo Scientific, USA Mini Sub Cell GT, BIO-RAD, USA
Falcon Tubes	EasyOpen 50-ml Centrifuge Tubes, JETBIOFIL, USA
Fly Pad	Fly Stuff, USA
Fly vials and closures	Fly Stuff, USA
Foot Valve	Fly Stuff, USA
Heat Block	Grant, UK
Hood	IP44/I, Wesemann, Germany
Incubator (18 °C)	WTW TS 606-G/4-i, Carl Stuart Limited, Ireland
Incubator (37 °C)	Nuve EN-120, AML, Belgium

Table 3.15. Equipment used in this thesis (continued).

Magnetic Plate	Agencourt SPRIPlate 96R ring magnetic plate, Beckman Coulter Genomics, USA
Microcentrifuge Tubes	1.5-ml Boil-Proof Microtubes, Axygen, USA 0.5-ml Thin Wall Flat Cap PCR tubes, Axygen, USA
Microwave	Arçelik, Turkey
Shaking Water Bath	GFL, 1083, Labfish, Germany
Stereomicroscope	S8APO, Leica, Germany
Thermocyclers	TC-512, Techne, UK RoboCycler 40 PCR Machine, Stratagene, USA
Tips	1000 µl, 200 µl, 100 µl, 10 µl Universal Fit Filter Tips, Axygen, USA
Vortex	Fisons WhirliMixer, UK
Water Purification	Arium® 611UV Ultrapure Water System, Sartorius, Germany

4. METHODS

The methods, applied in this study, will be categorized under two sections. The first section consists of the construction of the targeting vector, the second section consists of fly crosses that are required to replace the targeted gene with the transgene. The experiments in the first section were performed at Dr. Reenan's Lab at Brown University, the second section was carried out at NDAL.

4.1. Construction of The Targeting Vector

The targeting vector, P[w25.2], has the following specific elements that are utilized for the accomplishment of HR (Figure 3.3):

- p-elements that are required for p-element insertion of transgene in the fly genome in a random manner.
- Flippase Recognition Target (FRT) sites that are required for Flippase (FLP)-FRT excision of the transgene from its initial insertion place.
- I-*Sce*I recognition sites that are required for linearizing the circular extrachromosomal donor DNA that is generated by FLP-FRT excision.
- loxP sites are required for removing the mini-white gene by Cre-loxP site-specific recombination.
- Mini-white gene which is the marker for tracing of the transgene by screening for red eye color.
- Two distinct polylinker sites that are required for the insertion of homology arms.

4.1.1. PCR Amplification of dSOD Homolog Arms

Homologous recombination first involves the building of the targeting vector that contains two homologous arms specific to the gene of interest. For that purpose, two homolog arms were generated by PCR. PCR primers were designed by using the UCSC Genome browser (http://genome.ucsc.edu/). Each homolog arm was aimed to span ~2.5 kb of DNA and start and end in areas outside of the coding sequence. Also, these homolog

arms were centered across a non-conserved dispensable region that can be replaced by 76 bp of vector sequence (explained in detail later) (Figure 4.1). Additionaly the arms were designed in a way that they were free of the restriction enzyme sites that were used to insert the arms in the P[w25.2] vector (Figure 3.2).

The amplification of each arm was accomplished by the addition of 100 ng of *Drosophila* genomic DNA (gDNA), template to PCR reagents (Table 4.1). gDNA was kindly provided by Cynthia Staber from Dr. Reenan's laboratory. Homolog arms were amplified by their specific primers (Table 3.10) that include the necessary restriction enzyme recognition sites at the 5' and 3' ends (*Not*I and *Acc*65I or *Bsi*WI and *Asc*I) and by their specific reaction conditions as follows:

Table 4.1. PCR reagents used for the amplification of homolog arms.

Reagent	**Volume (µl)**	**[Stock]**	**[Final]**
Buffer	10	5X	1X
dNTP	1	10 mM	0.2 mM
Forward Primer	2.5	10 µM	0.5 µM
Reverse Primer	2.5	10 µM	0.5 µM
Phusion Taq	0.25	2U/µl	0.01U/µl

Arm1:

Initial denaturation:	98 °C	2 minutes	
Denaturation:	98 °C	30 seconds	40 cycles
Annealing:	64 °C	45 seconds	
Extension:	72 °C	1 minute	
	66 °C	2 minutes	
Final Extension:	72 °C	7 minutes	

Arm2:

Initial denaturation:	98 °C	2 minutes	
Denaturation:	98 °C	30 seconds	40 cycles
Annealing:	67 °C	30 seconds	
Extension:	72 °C	105 seconds	
	66 °C	2 minutes	
Final Extension:	72 °C	7 minutes	

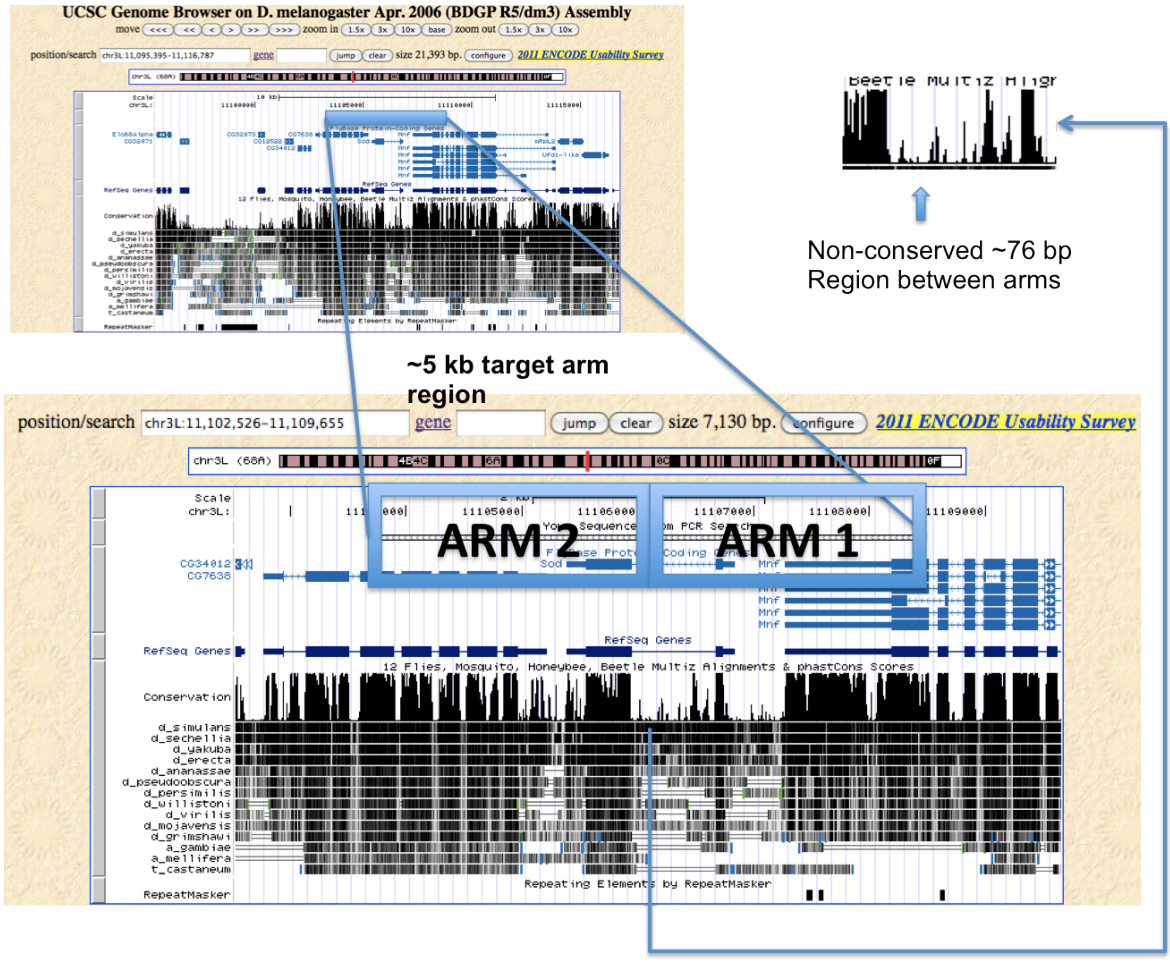

Figure 4.1. Designing of the homology arms using UCSC Genome Browser.

4.1.2. Identification and Purification Of PCR Products (homolog arms)

PCR products were analyzed on a 0.8% agarose gel which was prepared by dissolving 0.8 g of agarose in 100 ml 0.5X TBE buffer. The mixture was boiled in the microwave, until the agarose dissolved homogenously in the TBE and the solution became clear. After the agarose solution was cooled approximately to 60 °C, the intercalating dye EtBr was added to a final concentration of 0.5 µg/ml to enable visualization of DNA under UV light. Then, an 8-well comb was inserted and the homogenous mixture was poured onto it and left to polymerize at room temperature under the hood.

The PCR reactions were tested on the agarose gel. A 10 µl aliquot of the 50 µl PCR product was mixed with 6X loading dye to a final concentration of 1X. The polymerized gel was removed from the electrophoresis plate without the comb and placed into an electrophoresis tank containing 0.5X TBE. The DNA samples were loaded into the wells and the gel was first allowed to run at 45 Volt for 10-15 minutes and then at 70 Volt for ~35 minutes. The gel was visualized under UV light and documented. After observing the desired DNA bands under UV light, the remaining PCR products were eventually loaded on another 0.8% agarose gel and allowed to run. The gel slices that were containing the correct bands (~2.5kb) were cut out with the help of a razor under UV light.

The homology arm PCR products were purified from agarose gel with Promega Wizard® SV Gel and the PCR Clean-Up Kit:

- Each gel slice was placed in a 1.5-ml microcentrifuge tube and the tube was weighed using the balance.
- 10 µl membrane binding solution was added per 10 mg gel slice. The mixture was vortexed and incubated at 65 °C until the gel was completely dissolved.
- SV minicolumn, which is provided in the kit, was inserted into collection tube.
- Dissolved gel mixture was transferred to the minicolumn and incubated at room temperature for 2 minutes.
- After incubation, the mixture was centrifuged at 14,000 x g for 1 minute.
- The liquid in the collection tube was discarded and again the minicolumn was inserted back into it.

- 700 µl of membrane wash solution (with ethanol) was added into the minicolumn and the centrifugation step was repeated.
- The liquid in the collection tube was discarded and the minicolumn was inserted into it.
- 500 µl of membrane wash solution (with ethanol) was added into the minicolumn and the centrifugation step was repeated for 5 minutes.
- Again the liquid in the collection tube was discarded and the minicolumn was inserted into it.
- The empty minicolumn was centrifuged at 14,000 x g for 1 minute.
- Following the centrifugation, the minicolumn was transferred to a 1.5-ml microcentrifuge tube.
- 40 µl of nuclease-free water was added to the minicolumn and the minicolumn was incubated at room temperature for 1 minute.
- Upon incubation, the microcentrifuge tube was centrifuged at 14,000 x g for 1 minute.
- The minicolumn was discarded and the purified PCR product was kept at -20 °C for further experiments.

4.1.3. Cloning of Purified Homology Arm Products

Purified PCR product (e.g. Arm1) was ligated to TOPO cloning vector by Invitrogen, Zero Blunt® TOPO® PCR Cloning Kit:

- In a 1.5-ml microcentrifuge tube, 1.33 µl of freshly (1-2 days old) purified PCR product was mixed with 0.33 µl of salt solution and 0.33 µl of TOPO vector that are provided by the kit.
- The mixture was incubated at room temperature for 30 minutes.

After incubation, transformation with the ligation product was performed. XL1-Blue competent cells were thawed on ice. At the same time, 25 µl of Kanamycin and 85 µl of IPTG/X-GAL mixture were spread on LB-Agar plates. TOPO vector has Kanamycin resistance gene (Figure 3.1), thus kanamycin was used for ensuring the selective growth of

TOPO-harboring bacterial cells on the LB-Agar plate. Besides, IPTG/X-GAL mixture was used in order to facilitate blue/white screening for colonies that were carrying the recombinant plasmid, *i.e.* the TOPO vector that contains the PCR inserts. 100 µl of competent cells were carefully added to the ligation reaction and this mixture was kept on ice for 30 minutes, heat-shocked at 42 °C for 45 seconds and again kept on ice for 2 minutes. The mixture was spread on two LB-Agar plates in equal volumes (50 µl of the mixture for each plate); the plates were incubated overnight at 37°C.

4.1.4. Selecting Colonies For LB-Medium

By taking advantage of the aforementioned blue/white screening method, white colonies were picked-up from both plates (6 colonies for Arm1, 6 colonies for Arm2). For each colony, 3 ml LB-kanamycin was inoculated by picking the colony from the plate with the help of a toothpick and dropping the toothpick into a culture tube that contains the medium. Overall, 12 overnight-culture tubes were set up and incubated at 37°C in the shaking incubator.

4.1.5. Recovering Plasmid DNA From Overnight Cultures

Recovery of plasmid DNAs was performed with the Promega, PureYield™ Plasmid Miniprep Kit:

- 600 µl of each overnight culture was added to a 1.5ml microcentrifuge tube.
- 100 µl of cell lysis buffer was added to the microcentrifuge tubes and ingredients were mixed by inverting the tubes for 6 times.
- 350 µl of cold (4-8 °C) neutralization solution was added to the tubes and mixed thoroughly by inverting.
- The tubes were centrifuged at 14,000 x g for 3 minutes.
- The supernatant was transferred to a minicolumn, provided by the kit.
- The supernatant-containing minicolumn was placed into a collection tube and centrifuged at 14,000 x g for 15 seconds.

- The flow-through was discarded and the minicolumn was inserted into the same collection tube.
- 200 µl of endotoxin removal wash was added to the minicolumn and centrifuged at 14,000 x g for 15 seconds.
- 400 µl of column wash solution was added to the minicolumn and centrifuged at 14,000 x g for 30 seconds.
- After the washing steps, the minicolumn was transferred into a 1.5-ml microcentrifuge tube and 30 µl of elution buffer was added to it.
- The microcentrifuge tube was incubated at room temperature for 1 minute and centrifuged at 14,000 x g for 15 seconds to elute DNA.

The purified plasmids were checked for the presence of homolog arms by restriction digestion with *Eco*RI:

Recovered plasmid DNA:	1 µl
*Eco*RI:	1 µl
10X NEBuffer *Eco*RI:	1 µl
H_2O:	7 µl
Total:	10 µl

The digestion reaction was incubated at 37 °C for 1 hour. After the incubation, the digested DNA (6 DNA samples for Arm1, 6 DNA samples for Arm2) was run on a 0.8% agarose gel (Section 4.1.2.). When migration was completed, the gel was visualized under UV light. Because the vector contains *Eco*RI restriction sites flanking the TOPO regions (Figure 3.1), the plasmids that contain the insert are expected to release a ~2.5kb DNA fragment upon the *Eco*RI restriction digestion, indicating the successful insertion of the homolog arms. Hence the plasmids that showed such a restriction profile were chosen for the next sequencing analysis.

4.1.6. Sequence Analysis of Homology Arms

Because homologous recombination methods heavily relies on the sequence similarity of each arm to the corresponding regions in the genome, the homolog arms must be error-free or at least contain only synonymous changes in order to make HR possible. Therefore, each of the TOPO clones with correct restriction profiles was sequenced to verify that no base changes occurred during PCR amplification in the homology arms.

Sequencing of the homology arms were performed using the Applied Biosystems, BigDye® Terminator v3.1 Cycle Sequencing Kit. In the sequencing reaction, the following primers were used: TOPO-specific T7 and Sp6; Arm1-specific Seq 1, Seq 1R, Seq 2 and Seq 3; Arm2-specific Seq 3.5, Seq 4, Seq 5 and Seq 6 (Table 3.12). Insert specific sequencing primers were designed so that the sequencing covers homolog arms, especially the regions that correspond to the coding sequence of the gene of interest.

Table 4.2. Reagents used for Big Dye Sequencing.

Reagent	**Volume (µl)**	**[Stock]**	**[Final]**
Big Dye Buffer	2	10X	1X
Primer	2	10µM	1µM
Big Dye	2	-	-

The sequencing reaction was performed by the addition of 100 ng of DNA to the reagents provided in the Sequencing Kit with following cycle conditions:

Hot start:	94 °C	2 minutes	
Denaturation:	96 °C	10 seconds	25 cycles
Annealing:	50 °C	5 seconds	
Extension:	60 °C	4 minutes	

Following the Big Dye Sequencing reaction, the sequencing products were cleaned from the unincorporated nucleotides and other contaminants with the help of CleanSeq magnetic beads and Agencourt SPRIPlate 96R-Ring Magnet Plate:

- 6 µl of CleanSeq magnetic beads was added to each sequencing reaction tube.
- 80% ethanol was prepared freshly and 80 µl of this solution was also added to the reaction tube and mixed by pipetting.
- The reaction tubes were placed on the magnetic plate and incubated for 5 minutes.
- After the incubation, ethanol was removed by using a pipette.
- 150 µl of 80% ethanol was added to the tubes and mixed by pipetting.
- Ethanol was removed by again a pipette and the tubes were kept under the hood with their caps open for 10 minutes.
- 40 µl of water was added to tubes and vortexed until the magnetic beads were suspended back in the solution.
- The tubes were placed on the magnetic plate and incubated for 5 minutes.
- For each tube, 20-µl aliquot was taken and transferred to a clean strip tube for shipment.

The sequencing analysis was performed at the sequencing facility at the University of Wisconsin Biotechnology Center.

4.1.7. Construction of P[w25.2] Targeting Vector With Wild-Type Homolog Arms

After the sequencing results were received and the homolog arm sequences were verified that they had no mutations, the homolog arms were recovered from the TOPO vector by restriction digestion. As mentioned in Section 4.1.1, each homolog arm was designed to bear a specific pair of flanking restriction sites (*Asc*I/*Bsi*WI for Arm1 and *Not*I/*Acc*65I for Arm2); therefore, the homolog arms were released from the TOPO vector by digesting with the corresponding enzyme pair.

If one of the homology arms contains an endogenous restriction site similar to those flanking the other arm, then the insertion of the homology arms into the targeting

vector, P[w25.2], needs to be performed sequentially in such a way that the arm containing the endogenous site is cloned one after the other. In this study, first, Arm1 was released from TOPO and ligated to the vector, though neither arm had endogenous sites used for cloning the other arm—therefore, the cloning order was irrelevant.

Arm1 was flanked with *Bsi*WI and *Asc*I restriction sites and Arm1-containing TOPO vector was digested as follows:

DNA:	3 µl
*Asc*I:	1 µl
10X Multi core buffer:	3 µl
H_2O:	23 µl
Total:	30 µl

The restriction digestion reaction was incubated at 37 °C for 1 hour. After the incubation, 1 µl of *Bsi*WI enzyme was added to the digestion reaction and incubated at 55°C for an additional 1 hour. Digested DNA was then run on a 0.8% agarose gel (Section 4.1.2.). The ~2.5-kb restriction fragment, corresponding to the homolog arm, was cut out the agarose gel and was purified with the Promega Wizard® SV Gel and PCR Clean-Up Kit (Section 4.1.2).

At the same time, the P[w25.2] vector was also digested with the same restriction enzymes and under the same conditions as Arm1. But additionally, after 2-hours of incubation, 1 µl of CIP enzyme was added to the vector digestion reaction to prevent the vector to self-ligate upon digestion. CIP-treated vector was incubated at 37 °C for 1 hour and the product was run on a 0.8% agarose gel. The linearized plasmid was cut out and purified from agarose gel with the Promega Wizard® SV Gel and PCR Clean-Up Kit. After obtaining the purified vector and the insert DNA, these two fragments were ligated with each other as follows:

Vector:	1 µl
Insert:	5 µl
10X T4 Ligase Buffer:	3 µl
T4 Ligase:	1 µl
H_2O:	20 µl
Total:	30 µl

In order to check the CIP-treatment and ligation efficiency, a ligation reaction (without the insert DNA) was also performed as negative control:

Vector:	1 µl
10X T4 Ligase Buffer:	3 µl
T4 Ligase:	1 µl
H_2O:	25 µl
Total:	30 µl

The reaction tubes containing the ligations were incubated at room temperature for 5 minutes and then at 16 °C overnight. The next day, these ligation products were used in transformation of the competent bacteria as follows:

- 100 µl of competent bacteria cells were added into each ligation reaction tube and incubated on ice for 1 hour.
- After incubation, the reactions were heat-shocked in a water bath at 42°C, for 45 seconds and they were replaced on ice for 2 minutes.
- 25 µl of Ampicillin was spread on each LB-Agar plate and then 50 µl of the cells was spread on the plate as well.
- The plates were incubated at 37°C overnight.

The following day, 8 colonies were picked in total from the plates containing the cells transformed with the actual vector-insert ligation products, and separate overnight-culture tubes containing 3 ml of LB-ampicillin, each one inoculated with an individual colony, were set up and the cultures were incubated at 37°C in the shaking incubator.

The following day, the plasmid DNA isolation was performed from the overnight cultures with the Promega, PureYield™ Plasmid Miniprep Kit and the recovered DNA was subsequently analyzed by trying to drop Arm1 out of the plasmid via restriction digestion with *Bsi*WI and *Asc*I. One of the plasmids that yielded a restriction fragment of the correct size (~2 kb) upon digestion was then used for the next sequencing reaction, junction sequencing. This step is necessary to ensure that the insert (Arm1) has been properly integrated into the plasmid and to verify the integrity of the *Sce*I/LoxP/FRT sites within the P[w25.2] vector (Figure 3.2). Junction sequencing was performed using the Big Dye sequencing reactions with the junction-sequencing-specific primers (Table 3.13) and under the same conditions as described in Section 4.1.6. Similarly, the sequencing analysis was done by the sequencing facility at the University of Wisconsin Biotechnology Center.

After verifying that the clone had proper junctions on the plasmid, it was then used as a vector, this time, for the second round of arm cloning. Since Arm2 has flanking restriction sites for *Not*I/*Acc*65I, the vector was linearized with both of these enzymes:

DNA:	3 µl
*Not*I:	1 µl
*Acc*65I:	1 µl
10X Buffer 3:	3 µl
10X BSA:	3 µl
H_2O:	19 µl
Total:	30 µl

The restriction digestion reaction was incubated at 37 °C for 1 hour. After incubation, 1 µl of CIP enzyme was added to the vector digestion reaction and incubated at 37 °C for 1 hour. The vector was run on a 0.8% agarose gel, the linearized DNA was cut

out of the gel and purified with the Promega Wizard® SV Gel and PCR Clean-Up Kit. Wild-type Arm2 containing TOPO clone was also digested with the same enzymes, and similarly it was run on a 0.8% agarose gel, the DNA fragment corresponding to the homolog arm was cut out and purified from agarose gel with Promega Wizard® SV Gel and PCR Clean-Up Kit. After getting the purified vector and insert DNA, the two fragments were ligated with each other, the ligation product was used to transform competent bacteria cells and the amplified plasmid was recovered by performing the mini-prep steps as mentioned previously. After confirming the successful cloning of Arm2 into the vector by a restriction digestion with *Not*I/*Acc*65I, three separate digestion reactions were set up with the positive clone: *Bsi*WI/*Asc*I digestion to ensure the presence of Arm1, *Not*I/*Acc*65I digestion to ensure the presence of Arm2 and the following *I-Sce*I digestion to ensure the presence of both arms and the mini-white gene (Figure 3.3):

DNA:	2 µl
*I-Sce*I:	1 µl
10X NEBuffer *I-Sce*I :	1 µl
10X BSA:	1 µl
H_2O:	5 µl
Total:	10 µl

The *Bsi*WI/*Asc*I and *Not*I/*Acc*65I digestions were performed as previously described and the *I-Sce*I digestion was incubated at 37 °C for 1 hour before the gel-electrophoresis analysis.

A positive clone, that yielded the restriction fragments with the correct sizes after each digestion reaction was then sequenced for verification of the junctions between Arm2 and the vector (see Table 3.13 for the specific primers) under the same conditions with the Arm1 junction sequencing (described above). According to the sequencing results, a clone with good junctions was re-transformed into the competent bacteria for amplification and growing larger amounts of it. One of the homogenous colonies was then picked from the LB-Agar plate and inoculated in 50 ml of LB-ampicillin overnight-culture. The following day, plasmid purification was performed with Promega, PureYield™ Plasmid Miniprep

System and previously mentioned digestion verifications (with *Bsi*WI/*Asc*I, *Not*I/*Acc*65I and *I-Sce*I) of the purified DNA were repeated prior to sending it out for injection.

4.1.8. Construction of P[w25.2] Targeting Vector With Mutated Homolog Arms

Based on the computational analysis of dSOD, it was concluded that both of the *Drosophila* mutations that correspond to G37R and H48R in human SOD1 would localize in Arm2. Therefore in construction of the targeting vector with mutated homolog arms, Arm1 was kept as wild-type and each desired mutation was individually introduced to Arm2 with the Stratagene, QuickChange XL Site-Directed Mutagenesis Kit. Briefly, two complementary mutagenic primers (Table 3.11) were annealed to the denatured wild-type Arm2 bearing TOPO plasmid template and extended via a *Pfu*-polymerase. Following amplification, subsequent digestion of the reaction with *Dpn*I was performed to digest the parental DNA template and to select for mutation-containing synthesized DNA. The remaining reaction is transformed into competent cells and the resulting colonies were prepared as with the initial Topo clones (Section 4.1.5) and sequenced (Section 4.1.6). After sequence verification, mutated Arm2 was cloned into wild-type Arm1 carrying P[w25.2] vector by following the same steps as in the case for wild type Arm2 cloning and submitted for injection (Section 4.1.7).

The reaction condition for site-directed mutagenesis amplification was as follows:

Initial Denaturation:	95 °C	1 minute	
Denaturation:	95 °C	50 seconds	18 cycles
Annealing:	60 °C	50 seconds	
Extension:	68 °C	6 minutes	
Final Extension:	68 °C	7 minutes	

4.2. Fly Crosses

4.2.1. Maintenance of The Flies

The fly stocks were kept at 23-25°C. For collecting virgins, the vials were kept at room temperature during the daytime (9 a.m. to 6 p.m.) and at 18°C after 6 p.m. to 9 a.m. The vials were checked 3-times in a day for collecting virgins.

4.2.2. Excision of The P[w25.2] Construct And Initiation Of HR

Injection of the constructed targeting vector(s) into *Drosophila* embryo was achieved commercially in order to obtain transgenic flies with the constructs of interest. Since the construct is randomly integrated in the fly genome by P-element transformation, it is essential to excise the transgene from the integration site and target it to the gene of interest in the fly genome. This targeting event was achieved by crossing the transgenic flies to specialized fly lines (Figure 4.2). The flies used in this study were all *white* mutants, hence had white eyes under normal conditions and since the presence and expression of the mini-white gene ensures red eye color in the fly, mini-white gene in the targeting construct was used as an eye-color marker for tracing the transgene in the progenies of the subsequent crosses.

In the first cross (Figure 4.2):

- 50 transgenic male and 50 virgin female flies were collected. The females were expressing FLP recombinase and I-*Sce*I endonuclease under the control of a heat-shock promoter.
- 10 vials were numbered (1-10) and the crosses were set up in a way that each vial contained 5 males and 5 females.
- Parental flies were allowed to mate and lay eggs for three days. On the fourth day, parental flies were transferred to a new set of 10 numbered vials.
- The initial 10 vials containing fertilized eggs were taken and heat-shocked in a 38 °C shaking water bath for 1 hour. This heat-shock step ensures the expression of

FLP recombinase and I-*Sce*I endonuclease, thus the mobilization of the transgene. Heat-shock step was repeated after 24 hours.

- The parental flies in the second set of vials were let to lay eggs for two days and transferred to a new set of vials on the third day. The progeny was heat-shocked twice as described above.
- The parental flies in the third set of vials were let to lay eggs for two days and on the third day they were discarded. The progeny was heat-shocked twice as described above.
- In the end, there were 30 vials for each targeting construct (G37R and H48R) and each of them was heat-shocked twice at 38 °C for 1 hour.

The progeny of the first cross was screened for virgin females with white/mosaic eye color, which was considered as an indicator for the excision of the targeting construct from the initial insertion site. To continue with the second cross, 80-100 virgin females with white/mosaic eye color and straight wings were collected.

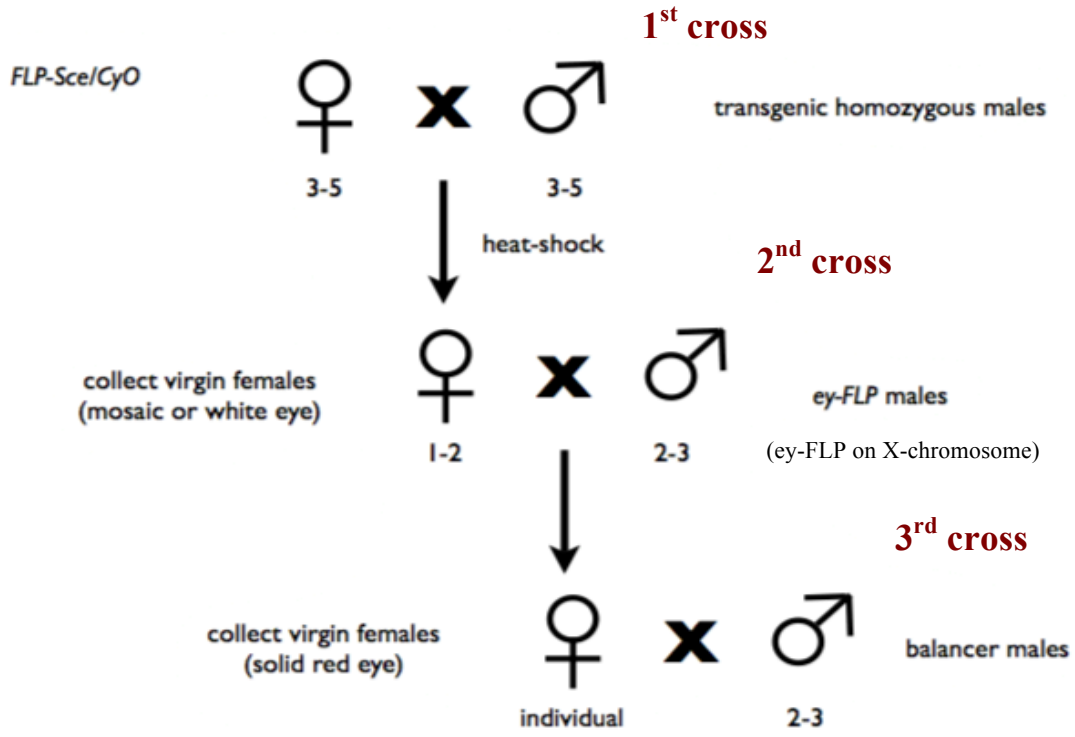

Figure 4.2. Overview of HR crossing scheme (Staber *et al.,* 2011).

4.2.3. Testing for The Potential Integration Via ey-Flp Crosses

In the second cross, two virgin females were crossed to one ey-Flp male, achieving 50 crosses at total for all transgenic lines. ey-Flp flies express FLP recombinase in their eye cells; therefore, this cross was done in order to discriminate the case that flies had the red-eye color since the transgene was removed from the integration site and HR was accomplished from the case that the flies had red-eye color due to the presence of the transgene in its initial integration site in the genome. The vials for this cross were labeled with their parental vial, *e.g.* crosses containing females from the parent vial 1, were labeled as 1.1, 1.2…. The progeny was then screened for red-eyed females in order to continue with the first validation step.

4.2.4. Validation of Integration By PCR

The red-eyed females collected from the previous step were individually crossed to w^{1118} males for establishing stocks. Vials were again numbered in a similar manner, *e.g.* 1.1.1 for a cross containing a female fly collected from vial 1.1 and 1.1.2 for the cross containing the other female fly collected from the same vial. After enough progeny arose from the above cross, gDNA extraction from these flies was performed, with the solutions in Table 3.3, as follows:

- 15 red-eyed flies were put in a 1.5-ml microcentrifuge tube and kept at -20 °C for 30 minutes.
- 200 µl of solution A was added into the tube and the flies were homogenized.
- The tube was placed on a heat block at 65 °C for 30 minutes. After 30 minutes, the tube was allowed to cool to room temperature.
- 400 µl of freshly mixed KOAc-LiCl solution was added and the tube was kept on ice for 10 minutes.
- After 10 minutes, the tube was centrifuged at 14,000 x g for 15 minutes.
- Supernatant was transferred to a clean 1.5-ml microcentrifuge tube and 600 µl of phenol:chloroform:isoamyl alcohol was added.
- The suspension was vortexed for 10 seconds and centrifuged at 14,000 x g for 1 minute.

- The supernatant was carefully transferred to a clean 1.5-ml microcentrifuge tube and 500 µl of chloroform was added.
- The suspension was vortexed for 10 seconds and centrifuged at 14,000 x g for 1 minute.
- The supernatant was carefully transferred to a clean 1.5-ml microcentrifuge tube and 350 µl of isopropanol was added onto it.
- The tube was inverted a few times to ensure the precipitation of the DNA and centrifuged at 14,000 x g for 15 minutes.
- Supernatant was removed and the pellet was rinsed with 400 µl of 70% ethanol.
- The tube was centrifuged at 14,000 x g for 10 minutes.
- Supernatant was removed and the pellet was air-dried.
- The gDNA was eluted in 75 µl of elution buffer.

The purified gDNA was then used as template, with specific primers designed to P[w25.2] vector and the flanking genomic sequence outside of Arm2 (Table 3.14), for pre-Cre PCR validation of Arm2 to ensure that the HR was successfully achieved. The PCR was run using the reactant with concentrations listed in Table 4.3 and with the following cycling conditions:

Table 4.3. pre-Cre PCR reagents.

Reagent	**Volume (µl)**	**[Stock]**	**[Final]**
10X *Taq* Buffer with $(NH_4)_2SO4$	2.5	10X	1X
dNTP	2.5	2 mM	0.2 mM
Forward Primer (ACC2)	1	10 µM	0.5 µM
Reverse Primer (SODVR2)	1	10 µM	0.5 µM
Taq Polymerase	0.25	5U/µl	1.25 U/µl

Initial Denaturation:	93 °C	3 minute	
Denaturation:	93 °C	20 seconds	40 cycles
Annealing:	64 °C	30 seconds	
Extension:	72 °C	2.5 minutes	
Final Extension:	72 °C	10 minutes	

Following amplification, PCR products were run on a 0.8% agarose gel (Section 4.1.2). Once the ~2.5kb DNA fragment was visualized under UV light, it was cut out and purified with the Qiagen, QIAquick Gel Extraction Kit:

- Gel slice was weighed in a 1.5-ml microcentrifuge tube.
- 10 µl Buffer QG was added per 10 mg gel slice. The tube was inverted for 3-6 times and incubated at 50 °C until the gel was completely dissolved.
- After the gel slice was dissolved, 1 gel volume of isopropanol was added to the sample and mixed.
- The mixture was transferred into QIAquick column and collection tube apparatus and centrifuged at 14,000 x g for 1 minute.
- The liquid in the collection tube was discarded and the column was inserted.
- 500 µl of Buffer QG was added into the column and the centrifugation step was repeated.
- The liquid in the collection tube was discarded and the column was inserted.
- 750 µl of Buffer PE (with ethanol) was added into the column and the centrifugation step was repeated.
- The liquid in the collection tube was discarded and the empty column was centrifuged at 14,000 x g for 1 minute.
- The column was inserted into a clean 1.5-ml microcentrifuge tube.
- 30 µl of elution buffer was added to the column and incubated at room temperature for 2 minutes.
- After incubation, the microcentrifuge tube was centrifuged at 14,000 x g for 1 minute ın order to elute the DNA.

The purified DNA was then sent to Refgen for sequencing (with same primers used in Table 4.3) in order to check the presence of the desired mutation.

4.2.5. Establishment of pre-Cre Stocks

Because dSOD gene is located on the third chromosome of the *Drosophila* genome, validated pre-Cre flies were crossed to flies that were carrying balancers for their third chromosome in order to establish pre-Cre stocks (Figure 4.2, third Cross). In this cross, flies carrying TM2/TM6B on their third chromosome were used and the progenies were screened for both red-eye color and the phenotype of TM6B, in order to select balanced mutant flies. Then, these flies were crossed with each other to get homozygous mutants.

4.2.6. Removal of The Mini-white Gene

In order to remove the mini-white gene from the targeted region, crosses of transgenic lines with Cre flies were utilized by taking advantage of the balancer switching approach (Figure 4.3). First, Cre recombinase expressing flies were crossed to TM2/TM6B flies and this time progeny was screened for white-eye color and the phenotype of TM2. White-eyed and TM2 bearing individual virgin females were then crossed to red-eyed and TM6B bearing individual males. The progeny was screened for white-eye color (indicating the removal of mini-white gene) and TM2 phenotype.

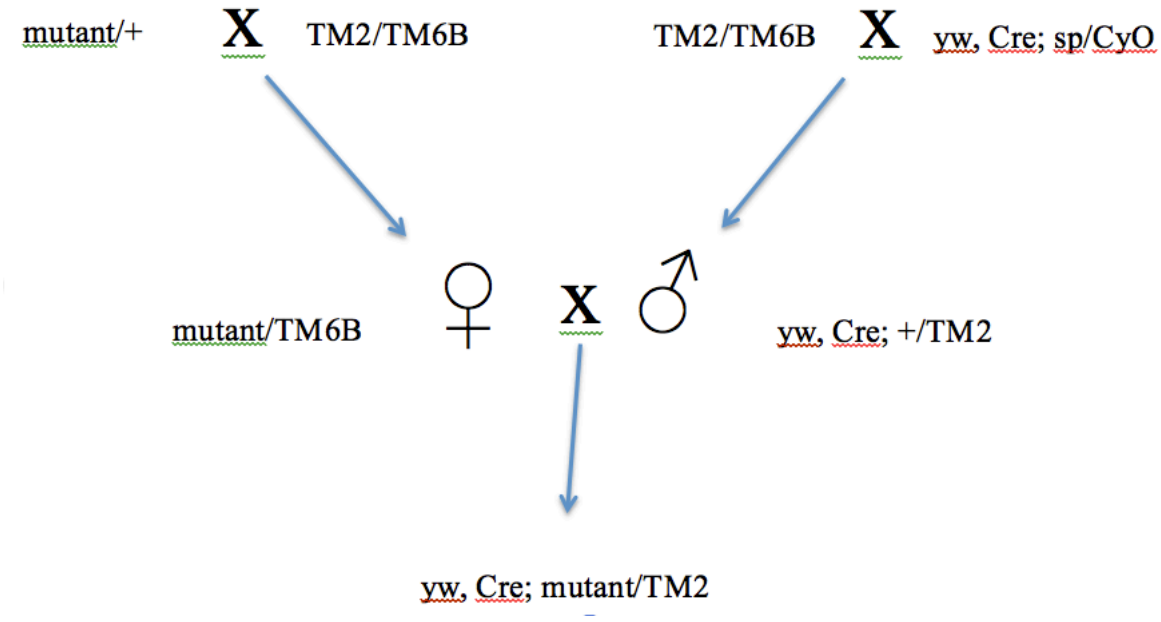

Figure 4.3. Schematic view of balancer switching method.

4.2.7. Post-Cre Validation

After collecting the progeny of the Cre expressing line and pre-Cre transgenic mutant lines, these flies were used for post-Cre validation PCR. This PCR was performed in order to confirm the removal of the mini-white gene; the following cycling conditions were applied:

Table 4.4. post-Cre PCR reagents.

Reagent	Volume (µl)	[Stock]	[Final]
10X HF PCR Buffer	2.5	10X	1X
dNTP	2.5	2 mM	0.2 mM
Forward Primer (SODVF2)	1	10 µM	0.5 µM
Reverse Primer (SODVR2)	1	10 µM	0.5 µM
HF Enzyme Mix	0.25	5U/µl	1.25 U/µl

Initial Denaturation:	93 °C	3 minute	
Denaturation:	93 °C	20 seconds	40 cycles
Annealing:	60.1 °C	30 seconds	
Extension:	68 °C	6 minutes	
Final Extension:	68 °C	15 minutes	

Because the primers were specific for the endogenous locus, the targeted and endogenous chromosomes cannot be distinguished from each other unless a restriction digestion was performed (Figure 4.4).

a.

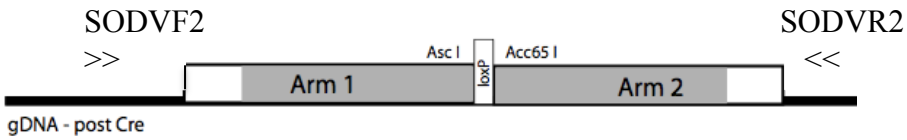

b.

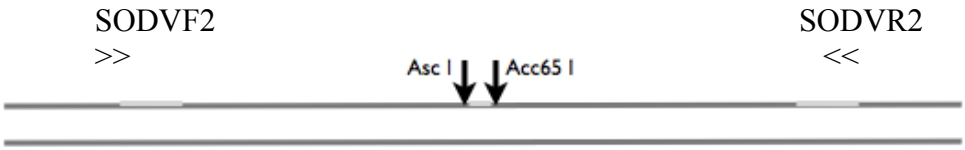

Figure 4.4. Distinguishing between the targeted and endogenous chromosomes: a. Post-Cre primers and targeted chromosome; b. PCR product of targeted chromosome (upper band), and endogenous chromosome (lower band) (Staber *et al.*, 2011).

5. RESULTS

5.1. Construction of The Targeting Vector

5.1.1. Analyzing The PCR-amplified Homology Arms From Genomic DNA

After amplification of the homology arms, the PCR products were run separately on a 0.8% agarose gel to confirm their sizes (Figure 5.1. and Figure 5.2.).

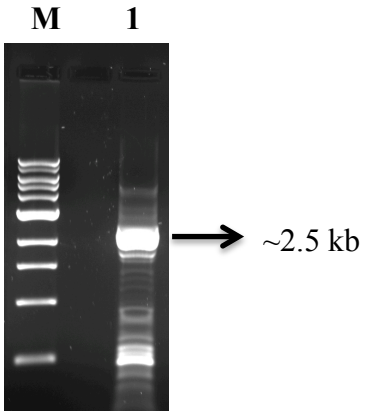

Figure 5.1. Agarose gel analysis of amplified Arm1
(M: 1kb DNA ladder (NEB); lane 1: Arm1 amplification product).

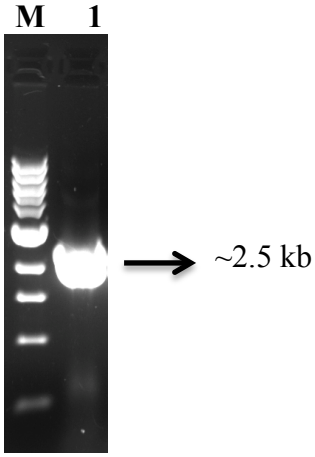

Figure 5.2. Agarose gel analysis of amplified Arm2 (M: 1kb DNA ladder (NEB); lane 1: Arm2 amplification product).

5.1.2. Restriction Digestion Verification Of Homology Arms In TOPO Vector

The presence of a homology arm in the TOPO vector was tested by an individual *Eco*RI digestion. The clones, that have the homology arm, yield a ~2.5-kb DNA band in the agarose gel analysis upon restriction digestion, however, since both homology arms include *Eco*RI restriction sites, the expected restriction profiles were different than this for each arm: Three fragments of ~950, 850, 650-kb for Arm1 and two fragments of ~1600 and 850-kb for Arm2 (Figure 5.3).

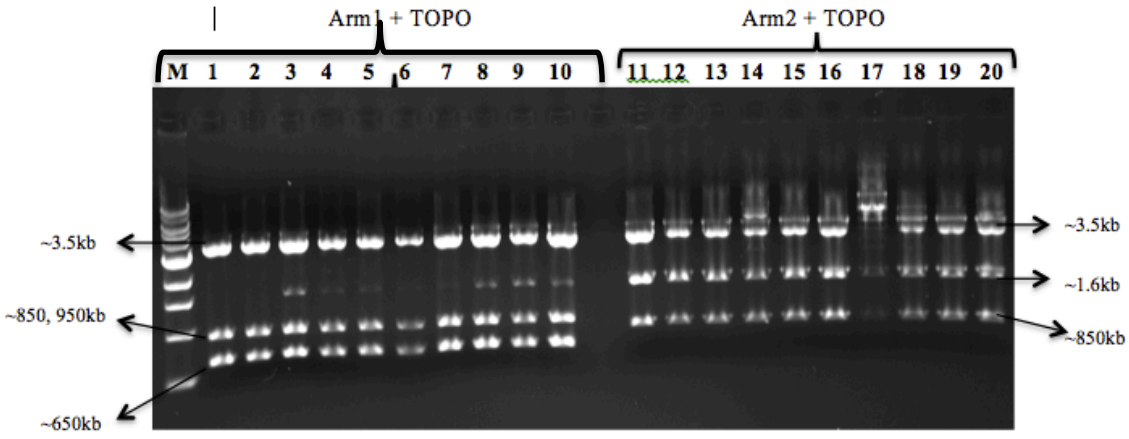

Figure 5.3. Digestion verification of homology arms in TOPO vector
(M: 1kb ladder (NEB); 1-10: digested, Arm1 harboring TOPO; 11-16 and 18-20: digested, Arm2, harboring TOPO; 17: undigested, empty TOPO).

5.1.3. Junction Sequencing Results For The Homology Arms

After ligating the homology arms into the P[w25.2] vector, all junctions were sequenced for each arm to confirm proper cloning and to check the presence of:

- SceI (5' TAGGGATAACAGGGTAAT 3'),
- lox-P (5' ATAACTTCGTATAATGTATGCTATACGAAGTTA 3')
- FRT (5' GAAGTTCCTATACTTTCTAGAGAATAGGAACTTC 3') sites.

Examples for the junction sequencing results are shown in Figure 5.4 for Arm1, and in Figure 5.5 for Arm2.

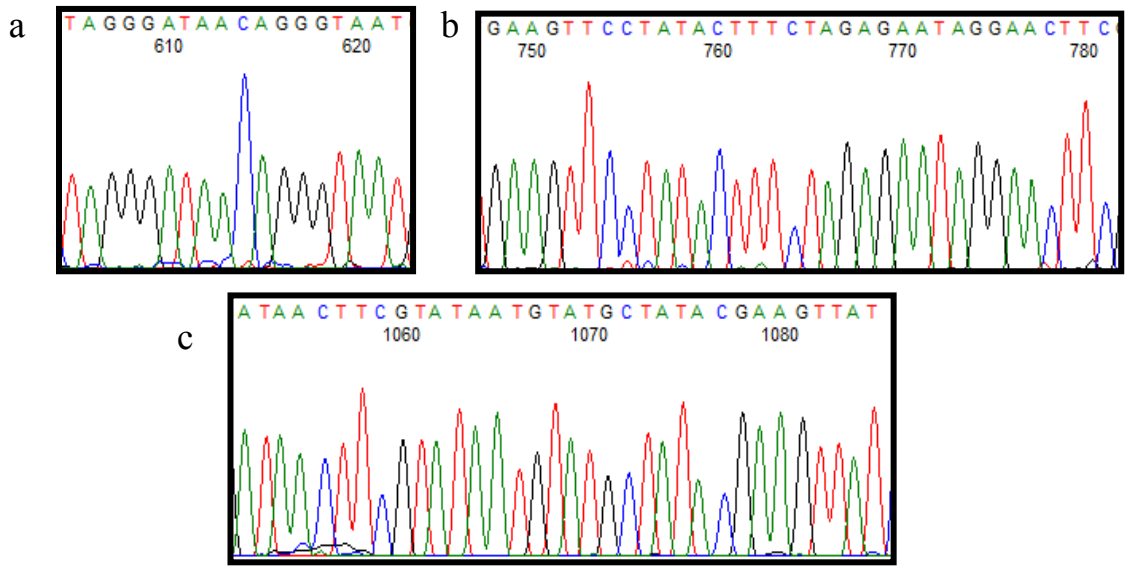

Figure 5.4 Junction sequencing chromatogram for Arm1: a. SceI site; b. FRT site; c.loxP. site

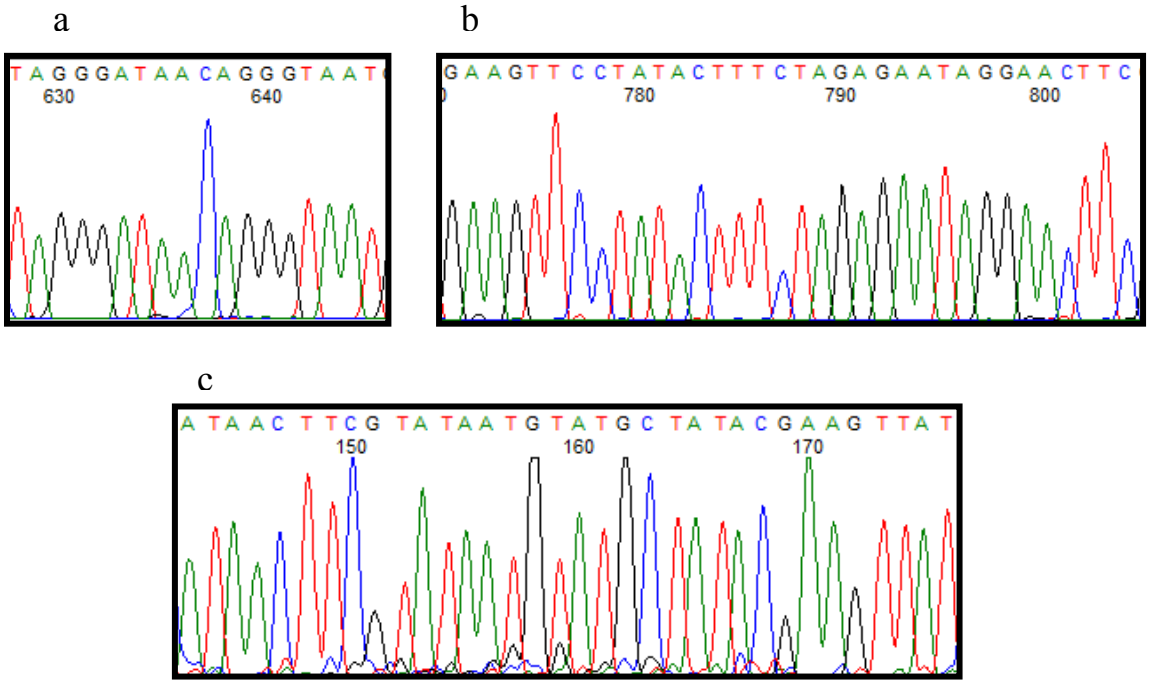

Figure 5.5 Junction sequencing chromatogram results for Arm2: a. SceI site; b. FRT site; c.loxP site.

5.1.4. Generation of The Mutated Arms By Site-Directed Mutagenesis

After performing site-directed mutagenesis to generate the desired mutations in the homology arms, the presence of each mutation was verified by sequencing. The mutation GGC→CGC corresponding to human G37R and the mutation CAC→CGC corresponding to human H48R are shown in Figure 5.6 and Figure 5.7.

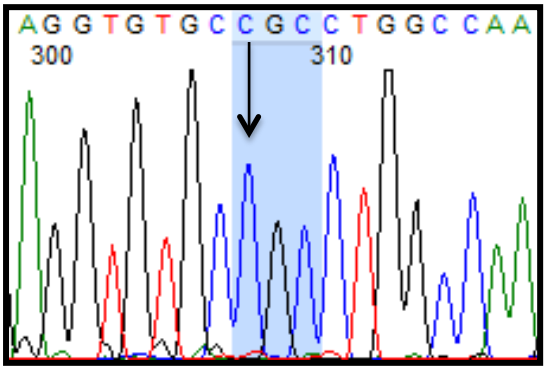

Figure 5.6. GGC→CGC transversion (Glycine → Arginine).

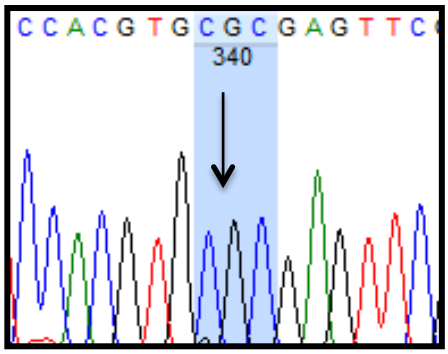

Figure 5.7. CAC→CGC transition (Histidine→Arginine).

5.1.5. Verification of Homology Arms In P[W25.2] Vector By Restriction Digestion

After successful cloning of both homology arms into the targeting vector, three separate digestion reactions were set up with the positive clones to verify the presence of both arms. An example is shown in Figure 5.8: M is the 1kb ladder (NEB), lanes 1 and 2 are *Sce*I digestion products, lanes 4 and 5 are *Not*I/*Acc*65I double-digestion products, lanes 6 and 7 are *Bsi*WI/*Asc*I digestion products. *Sce*I recognition sites are flanking the region that spans both homology arms and the ~5-kb mini-white gene (Figure 3.3.). Therefore,

*Sce*I digestion should give rise to restriction fragments of ~10 kb (two homology arms and the mini-white gene) and ~4 kb (linearized vector DNA). In this study, *Not*I/*Acc*65I recognition sites were present in the flanking region of Arm2, and *Bsi*WI/*Asc*I recognition sites were present in the flanking region of Arm1; thus double-digestion of the targeting vector with these enzymes yielded restriction fragments of ~2.5 kb (homology arm) and ~11.5 kb (linearized vector DNA), respectively (Figure 5.8).

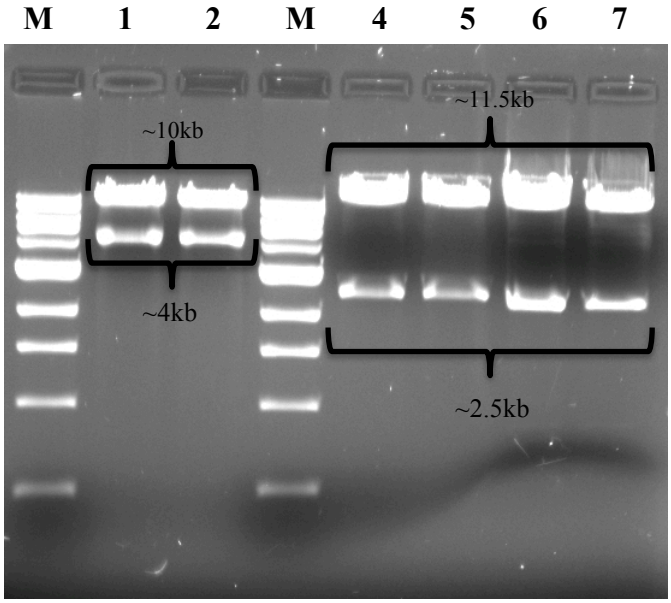

Figure 5.8. Verification of homology arms in P[w25.2] vector by restriction digestion.

5.2. Fly Crosses

Upon microinjection of each targeting vector (wild type, G37R and H48R) into *Drosophila* embryos, several fly crosses were performed to achieve the successful targeting of the dSOD gene. After the first two crosses, shown in Figure 4.2., and ensuring the persistence of the progeny by another cross, the progeny was validated by PCR and sequencing. Positive fly lines were taken to subsequent crosses and the pre-Cre stocks were established for these lines. Another validation through PCR amplification and subsequent restriction digestion of the PCR-product was performed following the removal of the mini-white gene, and the positive lines were kept as post-Cre stocks.

5.2.1. Pre-Cre PCR Validation And Stock Establishment

Among three transgenic lines, the wild-type line did not yield the required female progeny with white or mosaic eye-color after the 1st cross; therefore, it was not used for the subsequent crosses. Crosses with either G37R or H48R lines were accomplished, and according to pre-Cre PCR results successful targeting of dSOD gene was achieved for both mutations (Figure 5.9).

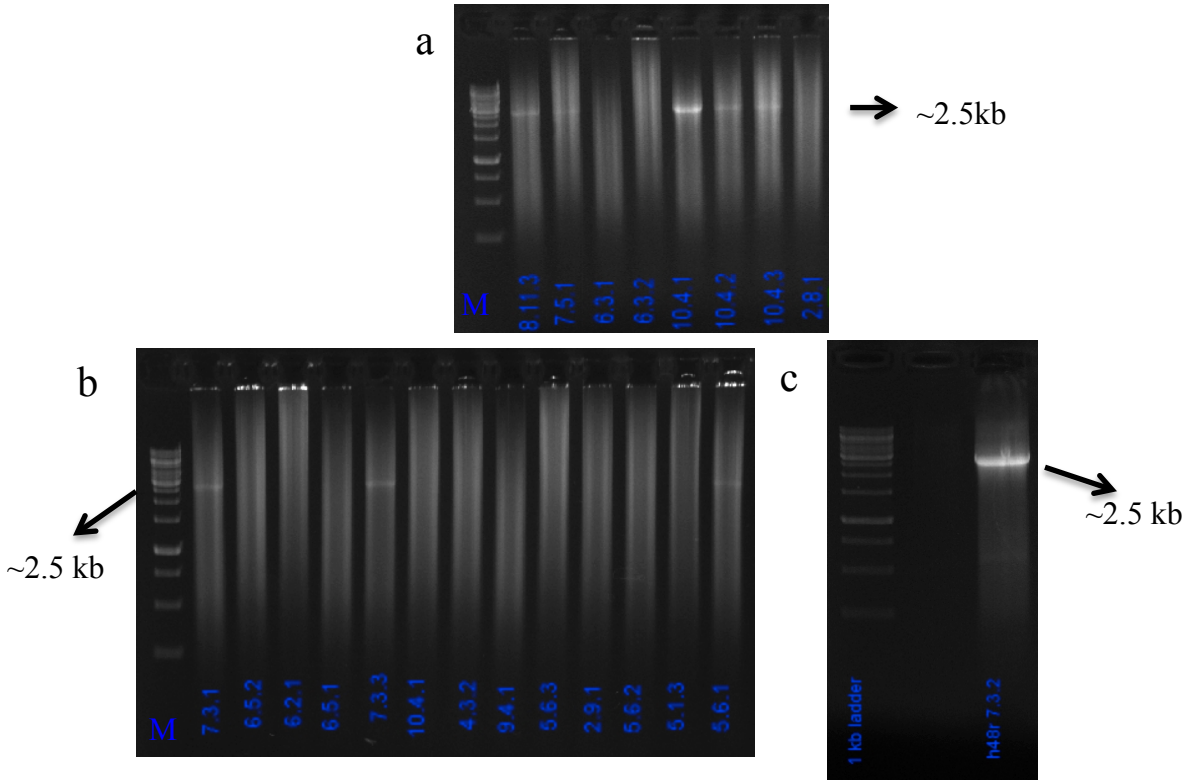

Figure 5.9. pre-Cre validation of G37R and H48R mutant flies for Arm2:
a. amplification results for G37R; b. amplification results for H48R; c. H48R mutant candidate; M: 1-kb ladder (Fermentas).

15 candidates for G37R-mutant flies were screened by PCR; an example of the validation result is shown in Figure 5.9.a. Samples labeled as 7.5.1, 8.11.3, 10.4.1, 10.4.2 and 10.4.3 produced the desired PCR product indicating the presence of Arm2 and were taken to further analysis by sequencing. The remaining candidates were negative for the presence of Arm2 and they were eliminated.

14 candidates for H48R-mutant flies were screened by PCR and the related results are shown in Figure 5.9.b-c. Samples labeled as 5.6.1, 7.3.1, 7.3.2 and 7.3.3 were positive for the presence of Arm2, they were analyzed for the desired mutation by sequencing.

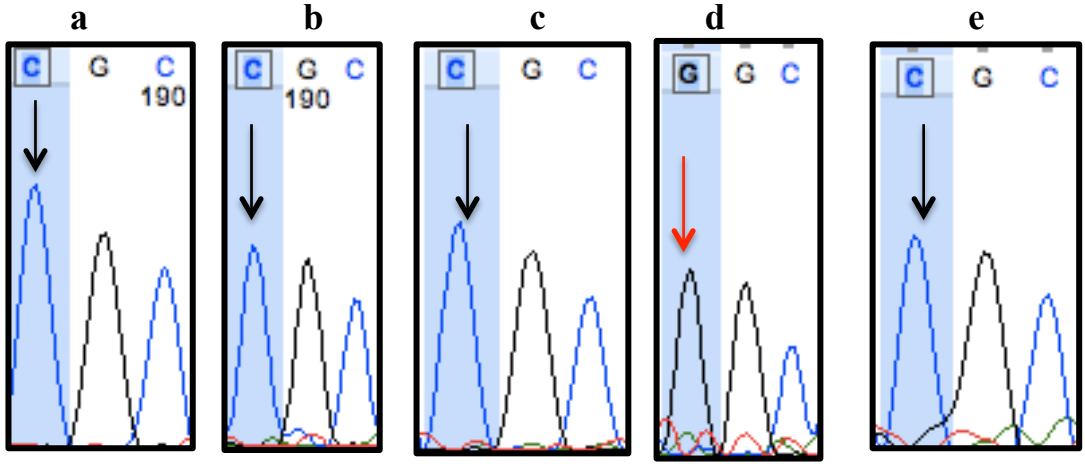

Figure 5.10. Sequencing analyses of G37R-mutant candidates: a. 7.5.1; b. 8.11.3; c. 10.4.1; d. 10.4.2; e. 10.4.3.

Sequencing analyses of five G37R-mutant candidates confirmed the presence of the desired mutation in four of the candidates, whereas the remaining one was found to be wild type for *dSOD* and hence kept as a control for the study.

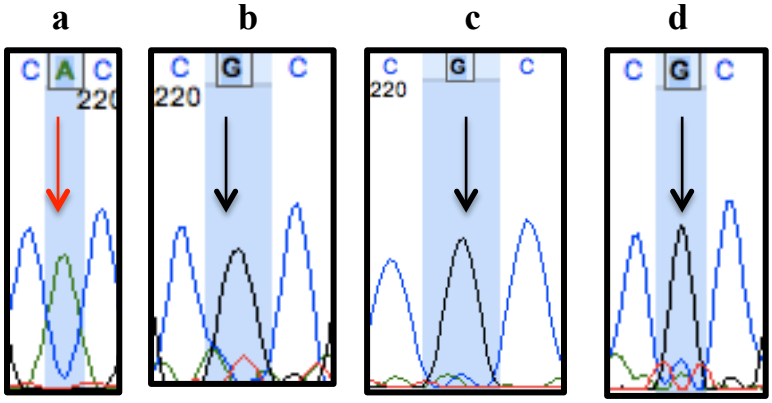

Figure 5.11. Sequencing analyses of H48R-mutant candidates: a. 5.6.1; b. 7.3.1; c. 7.3.2; d. 7.3.3.

Sequencing analyses of four H48R-mutant candidates confirmed the presence of the desired mutation in three of the candidates, whereas the remaining one was found to be wild-type for *dSOD;* it has also been kept as a control for the study.

In the beginning of the study, when the homology arms were sequenced after the site-directed mutagenesis step, a non-synonymous nucleotide change was found to be present on Arm2. This variation, resulting in N96K for dSOD, was further investigated by sequencing the corresponding position in different strains of *D. melanogaster* namely Canton S, Oregon R and w^{1118}. Sequencing revealed that this variation actually corresponded to a single nucleotide polymorphism, 288C/A, in *D. melanogaster* strains (Figure 5.12).

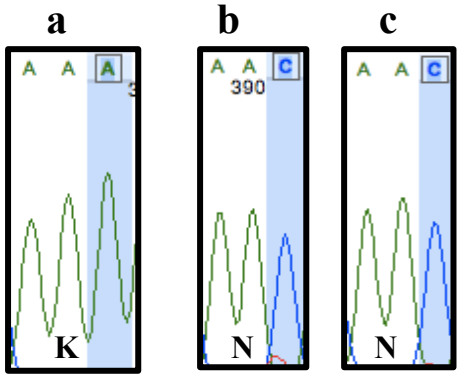

Figure 5.12. Sequencing results of three *D. melanogaster* species for 288C/A: a. Canton S; b. Oregon R; c. w^{1118}.

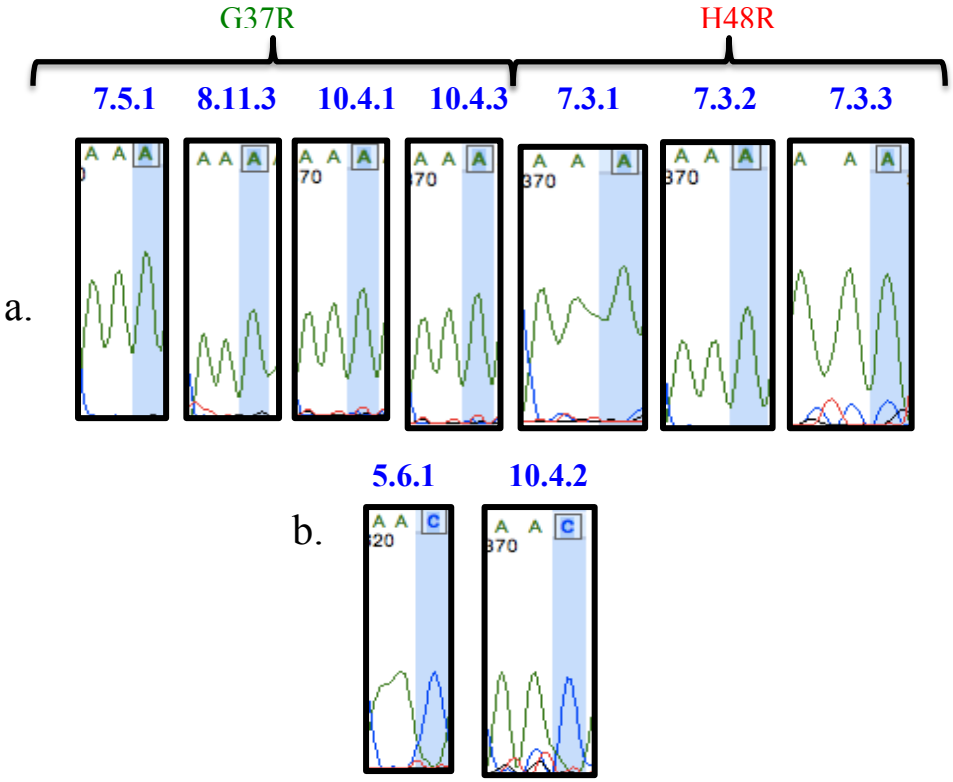

Figure 5.13. Sequencing results of targeted fly lines for 288C/A: a. mutant lines; b. control lines.

Sequencing analyses of G37R and H48R mutants also revealed that the mutant lines used in this study had the A-allele (Figure 5.13a.), while the controls had the C-allele for this polymorphic site (Figure 5.13b.).

5.2.2. Post-Cre PCR Validation And Stock Establishment

After establishing the pre-Cre stocks, these targeted lines were crossed to Cre recombinase expressing flies to ensure removal of the mini-white gene by Cre-loxP recombination.

PCR validation was performed for three H48R (labeled red) and four G37R mutant post-Cre lines (labeled green). Because primers for this step were *dSOD* specific and PCR product may occur from both the targeted and the endogenous chromosome, w^{1118} (labeled white) was used as the control sample for PCR (Figure 5. 14).

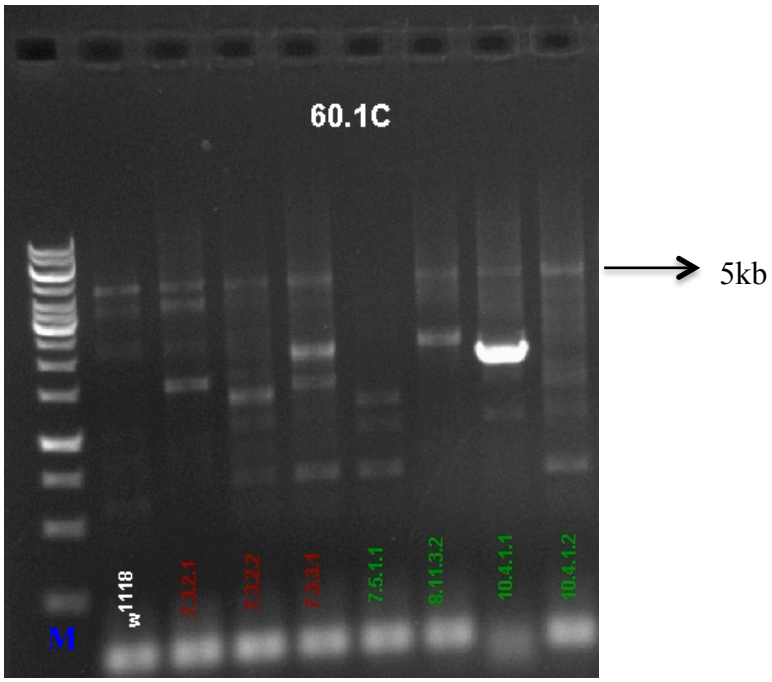

Figure 5.14. post-Cre PCR validation of three H48R and four G37R mutant lines, M: 1-kb ladder (Fermentas).

Following isolation of the 5-kb PCR products from the agarose gel, a restriction-digestion by *Asc*I was performed for one H48R and two G37R products. Since *Asc*I restriction site is on the downstream flanking region of Arm1 (Figure 3.3), *Asc*I cuts the 5-kb PCR product into two, Arm1 and Arm2, both ~2.5 kb in size (Figure 5.15). The desired restriction digestion profile was observed for one of the G37R products, where the expected 5-kb and 2.5-kb fragments were clearly visible in the agarose gel analysis (line 8.11.3.2 - Figure 5.15, lane 3). However, one of the remaining products had an unexpected restriction digestion pattern (with an extra ~2-kb fragment) and the other was insufficient in the amount for the agarose gel analysis (Figure 5.15, lanes 1-2).

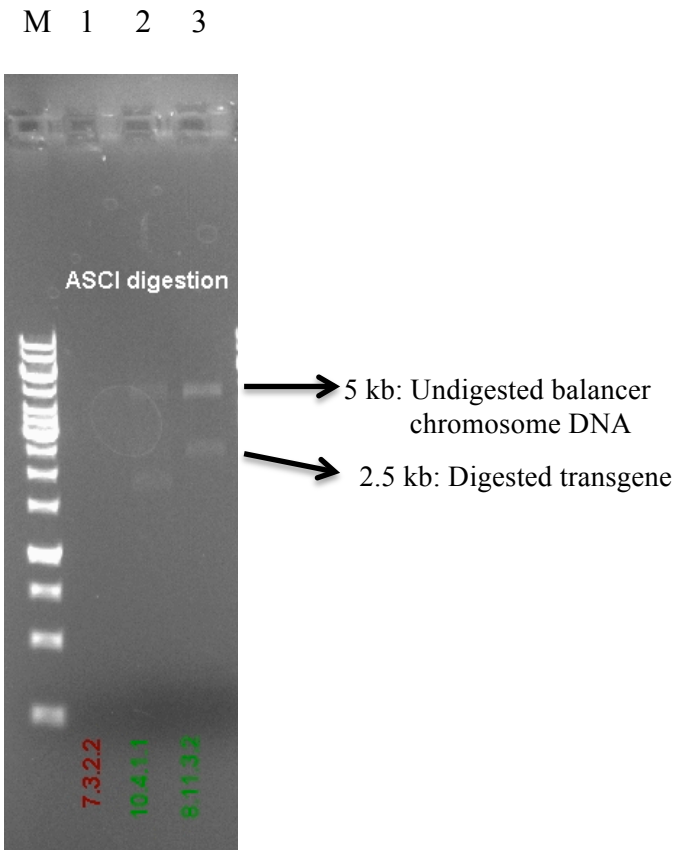

Figure 5.15 *Asc*I digestion verification, M: 1-kb ladder (Fermentas).

6. DISCUSSION

Neurodegenerative diseases have complex pathogenic mechanisms due to complex interactions between individual genetic background and environmental factors. Among all risk factors, the most important one is old age. The onset of NDs usually occurs in mid to late life, thus NDs are known as late-onset diseases (Farooqui and Farooqui, 2009). As NDs are becoming more common with the extending human life span, many studies have been done on these diseases to elucidate the underlying complex mechanisms.

Motor neuron diseases are a sub-group of NDs and ALS is the most prominent example. ALS is a late-onset disease and it involves degeneration of both upper and lower motor neurons. It is lethal 3-5 years after diagnosis and has no effective treatment. Mutations on the SOD1 gene, which encodes a highly conserved protein of 153 amino acids, are the major genetic causes underlying ALS and they are known to be dispersed throughout the gene. Both sporadic and familial forms of ALS have similar pathogenic mechanisms and, therefore, the elucidation of the genetic causes regarding familial cases is expected to shed light on the sporadic forms of the disease, which are much more common (Lu and Vogel, 2009).

Analysis of genes and pathways thought to be responsible for human diseases is hard to conduct, due to complex patterns of inheritance, lack of sufficient family pedigree data and population-based genetic heterogeneity. One powerful approach for studying ND mechanisms has been the use of animal models. Among various animal models, such as *C. elegans,* zebrafish, mice *etc.*, fly models stand as an excellent model to study NDs. Fruit flies, at first glance, may seem quite irrelevant for studying human biology, since the arthropod lineage –the phylum which contains the fruit flies– is thought to be separated from the vertebrate lineage more than 600 million years ago. (Hirth, 2010). This is, however, not true, many genes and biological pathways are conserved between humans and flies. Furthermore, it has been shown that 75% of human disease-linked loci have homologs in *Drosophila* (Reiter *et al.,* 2001). Along with many advantages of fruit flies for being appropriate laboratory animals (*e.g.* being small, cheap; having short reproductive

and developmental cycles etc.), their small, yet still complex brains make *Drosophila* an appropriate model organism for ND studies.

In this study the specific aim was to introduce two individual ALS-linked human *SOD1* mutations (G37R and H48R) into the dSOD gene. These mutations were chosen considering the fact that both amino acids at positions 37 and 48 have been conserved among many different species including *S. cerevisiae, A. thaliana, D. melanogaster* and humans (Figure 6.1). Also, these two mutations are phenotypically different from each other in the respect that G37R is a wild-type-like mutation, while H48R —along with the H48Q— is a metal-binding-region-specific lesion.

Figure 6.1. A portion of the multiple alignment of SOD1 that shows the conserved amino acids, G37 and H48 (http://www.ncbi.nlm.nih.gov/homologene/392).

6.1. Why Homologous Recombination?

In this study, instead of the widely used Gal4/UAS binary system for generating human disease models with flies, gene targeting was performed by homologous recombination. HR was preferred for its ability to introduce mutations with surgical precision into the endogenous locus, hence minimally perturbing the locus and maintaining the normal expression of the gene of interest. Basically, gene targeting by HR was accomplished in two steps: The first step involving the generation of the targeting construct and the second step consisting of the fly crosses in order to target the construct to the endogenous locus.

6.2. Construction of The Targeting Vector

Generation of the targeting construct begins with the designing of the homology arms. Homology arms should be designed in a way that, if possible, the desired mutations are located at the center of the arms to increase the likelihood of successful integration during HR. Also, it is important that the homology arms should not contain any other additional mutations than the desired one, since the overall phenotypic effect should only be the result of the desired mutation. In this study, apart from the two target constructs (one for G37R and one for H48R) bearing the wild type Arm1 and mutated Arm2, a targeting vector containing only the wild type homology arms was constructed as a control for the study in order to ensure that the whole method had no effect on expression or function of the targeted gene—potentially resulting in phenotypic abnormalities (Staber *et al.,* 2011).

Junction sequencing was also an important checkpoint during the generation of the targeting vector, since these sites are required to achieve a successful targeting during fly crosses (Figure 3.2). Junction sequencing was done to confirm proper cloning and the presence of *Sce*I, lox-P and FRT sites on the targeting vector (Figures 5.4 and 5.5).

After the injection of the targeting construct into *Drosophila* embryos, the vector was expected to be inserted into the fly genome by P-element transformation and to be

localized in a random manner. Therefore, several fly crosses were set in order to mobilize the transgene from its initial integration place and to target it to the endogenous locus (Figure 4.2).

6.3. Fly Crosses

In the first cross, flies that express yeast FLP recombinase and I-*Sce*I endonuclease under heat-shock promoter were crossed with the targeting-vector-harboring transgenic flies. Two-three days after mating, the fertilized eggs were heat-shocked in order to induce FLP and I-*Sce*I expression. When expressed, FLP acts on FRT sites that are present on the targeting vector and excises the sequence between the FRT sites (Figure 3.3.). The resulting circular molecule is then linearized by I-*Sce*I and may recombine at the endogenous locus by the homology arms.

One important feature in the targeting vector is the presence of the mini-white gene (Figure 3.2). Throughout the fly crosses, the mini-white gene was used as a marker, since the flies used in this study were all white mutants, i.e. they originally had white eye color instead of the red, wild type eye color.

After the first cross and heat-shock steps, the progeny was screened for white or mosaic eye color. The reason for this screening is that to achieve targeting of the gene of interest, the initial requirement is the excision and mobilization of the transgene. So, the desired F1 progeny are the ones in which excision was successful via FLP-FRT recombination. If the transgene would be mobilized, there would be no mini-white expression and the progeny will be either white (100% excision) or mosaic-eyed (partial excision). Indeed, this event must occur in the germ-lines of these F1 progeny in order to be propagated, but this cannot be checked until the next generation. Therefore, eye color is used as an indicator of the events that have possibly occurred in the germ cells.

Following the screen, among three transgenic lines (wild type, G37R and H48R), the wild type line did not yield the required female progeny with white or mosaic eye-color after the 1st cross. This might have resulted either from an inefficient FLP-FRT

recombination or from very low efficient excision of the targeting vector in germ cells. However the wild type fly line could be excluded from the subsequent crosses, because, it is well-known that, HR does not always result in 100% integration of the mutation carrying arms into the endogenous locus, thus the targeted fly is sometimes able to repair the mutation. Therefore, obtaining wild type targeted flies after pre-Cre validation by sequencing is very probable.

In the 2nd cross, the mosaic- and white-eyed virgin female progeny was crossed to ey-Flp males. As mentioned before, white or mosaic eye color in females does not necessarily indicate the excision of the transgene in the germ cells. If the transgene is never excised from its initial place in the germ cells of the fly, then the progeny will have red eye color due to the expression of the mini-white gene. If the transgene is mobilized and inserted into the target locus, then the progeny will have red eye color due to the expression of the mini-white gene. If the transgene is excised but not integrated into the genome, the eye color will be white due to the loss of the mini-white harboring transgene.

So, the 2nd cross was performed in order to discriminate between the progeny in which HR was successful and the progeny in which the excision was not successful; this was expected to leave the transgene in its primary insertion site. A cross with ey-FLP flies elucidates this complexity. ey-FLP flies express FLP recombinase only in their eyes. So, if the transgene is never excised, then it still has the flanking FRT sites on which FLP can act. The FLP effect on the FRT sites will excise the transgene between these sites and the progeny will have white eyes and be eliminated. But if the transgene is excised and inserted into the target locus, it will not be affected by FLP due to loss of FRT sites, hence it will remain intact and the progeny will be red-eyed.

6.4. Validation

After the 2nd cross, there were 15 red-eyed flies for G37R and 14 for H48R. These flies had the mini-white gene for sure, but in order to check if they were real mutants or not, these flies were validated by PCR, using one gene-specific and one vector-specific primer pair for Arm2 (Table 3.14). For five of the G37R and four of the H48R candidates,

Arm2 was successfully amplified, implying the transgene was localized into the target locus for these fly lines (Figure 5.9). The remaining lines were eliminated. These false-positive flies might be the ones in which the transgene could have been inserted in any other place than the target locus.

The sequencing results of the PCR-validated mutant-candidates revealed that one of the G37R and one of the H48R candidates were found to be wild type for dSOD gene and hence kept as controls. As expected, these two lines compensated for the wild type line which was eliminated in the beginning of the study. Also, these two control lines had the C-allele (Figure 5.13b) for the single nucleotide polymorphism, 288 C/A. Since the microinjection part of the study was performed commercially and the fly embryos were provided by the company, these lines might originally be the C-allele carriers. Moreover, the fact that the control lines also did not carry the desired mutation is likely to suggest an incomplete homologous recombination happening in these lines, therefore leaving the endogenous Arm2 region intact.

On the other hand, sequencing analysis revealed that four lines for G37R and three lines for H48R mutation candidates were positive for the desired mutations. Furthermore, these mutant lines had the A-allele for the single nucleotide polymorphism, 288 C/A, which indicates the successful integration of the mutated Arm2 into the endogenous locus (Figure 5.13a).

6.5. Near Future Goals

The aim of this study was to introduce two ALS-related human SOD1 mutations (G37R and H48R) into dSOD gene by homologous recombination. By several PCR validations and sequencing verifications, it was shown that these two mutations were successfully inserted into dSOD gene without causing any additional mutations in Arm2 by HR. But before considering these mutant flies as models to perform behavioral analyzes in ALS research, the mutant lines should be backcrossed to a wild type line for at least five generations in order to remove the balancers and cease the expression of the enzymes FLP, I-*Sce*I and Cre that are not naturally expressed by *D. melanogaster*.

REFERENCES

Alexianu, M. E., B. K. Ho, a H. Mohamed, V. La Bella, R. G. Smith, and S. H. Appel, 1994, "The role of calcium-binding proteins in selective motoneuron vulnerability in amyotrophic lateral sclerosis", *Annals of Neurology*, Vol. 36 (6), pp. 846-58.

Barber, S. C., and P. J. Shaw, 2010, "Oxidative stress in ALS: key role in motor neuron injury and therapeutic target", *Free Radical Biology & Medicine*, Vol. 48 (5), pp. 629-41.

Barmada, S. J., G. Skibinski, E. Korb, E. J. Rao, J. Y. Wu, and S. Finkbeiner, 2010, "Cytoplasmic mislocalization of TDP-43 is toxic to neurons and enhanced by a mutation associated with familial amyotrophic lateral sclerosis", *The Journal of Neuroscience :The Official Journal Of The Society For Neuroscience*, Vol. 30 (2), pp. 639-49.

Beleza-Meireles, A., and A. Al-Chalabi, 2009, "Genetic studies of amyotrophic lateral sclerosis: controversies and perspectives", *Amyotrophic lateral sclerosis :Official Publication Of The World Federation Of Neurology Research Group On Motor Neuron Diseases*, Vol. 10 (1), pp. 1-14.

Bento-Abreu, A., P. Van Damme, L. Van Den Bosch, and W. Robberecht, 2010, "The neurobiology of amyotrophic lateral sclerosis", *The European Journal Of Neuroscience*, Vol. 31 (chromosome 21), pp. 2247-2265.

Boillée, S., C. VandeVelde, and D. W. Cleveland, 2006, "ALS: a disease of motor neurons and their nonneuronal neighbors", *Neuron*, Vol. 52 (1), pp. 39-59.

Bruijn, L. I., 1998, "Aggregation and Motor Neuron Toxicity of an ALS-Linked SOD1 Mutant Independent from Wild-Type SOD1", *Science*, Vol. 281 (5384), pp. 1851-1854.

Cai, H. et al., 2005, "Loss of ALS2 function is insufficient to trigger motor neuron degeneration in knock-out mice but predisposes neurons to oxidative stress", *The*

Journal of Neuroscience : the official journal of the Society for Neuroscience, Vol. 25 (33), pp. 7567-74.

Capecchi, M. R., 1989, "Altering the genome by homologous recombination", *Science (New York, N.Y.)*, Vol. 244 (4910), pp. 1288-92.

Chan, H. Y., and N. M. Bonini, 2000, "Drosophila models of human neurodegenerative disease", *Cell Death And Differentiation*, Vol. 7 (11), pp. 1075-80.

Chen, Y.-Z. et al., 2004, "DNA/RNA helicase gene mutations in a form of juvenile amyotrophic lateral sclerosis (ALS4)", *American Journal Of Human Genetics*, Vol. 74 (6), pp. 1128-35.

Cheroni, C., M. Marino, M. Tortarolo, P. Veglianese, S. De Biasi, E. Fontana, L. V. Zuccarello, C. J. Maynard, N. P. Dantuma, and C. Bendotti, 2009, "Functional alterations of the ubiquitin-proteasome system in motor neurons of a mouse model of familial amyotrophic lateral sclerosis", *Human Molecular Genetics*, Vol. 18 (1), pp. 82-96.

Chow, C. Y., J. E. Landers, S. K. Bergren, P. C. Sapp, A. E. Grant, J. M. Jones, L. Everett, G. M. Lenk, D. M. McKenna-Yasek, and L. S. Weisman, 2009, "Deleterious variants of FIG4, a phosphoinositide phosphatase, in patients with ALS", *The American Journal of Human Genetics*, Vol. 84 (1), pp. 85–88.

Clement, a M. et al., 2003, "Wild-type nonneuronal cells extend survival of SOD1 mutant motor neurons in ALS mice", *Science (New York, N.Y.)*, Vol. 302 (5642), pp. 113-7.

Crapo, J. D., T. Oury, C. Rabouille, J. W. Slot, and L. Y. Chang, 1992, "Copper,zinc superoxide dismutase is primarily a cytosolic protein in human cells", *Proceedings Of The National Academy Of Sciences Of The United States Of America*, Vol. 89 (21), pp. 10405-9.

De Vos, K. J., A. J. Grierson, S. Ackerley, and C. C. J. Miller, 2008, "Role of axonal transport in neurodegenerative diseases", *Annual Review Of Neuroscience*, Vol. 31, pp. 151-73.

Devon, R. S. et al., 2006, "Als2-deficient mice exhibit disturbances in endosome trafficking associated with motor behavioral abnormalities", *Proceedings Of The National Academy Of Sciences Of The United States Of America*, Vol. 103 (25), pp. 9595-600.

Dion, P. a, H. Daoud, and G. a Rouleau, 2009, "Genetics of motor neuron disorders: new insights into pathogenic mechanisms", *Nature Reviews. Genetics*, Vol. 10 (11), pp. 769-82.

Dong, X.-xia, Y. Wang, and Z.-hong Qin, 2009, "Molecular mechanisms of excitotoxicity and their relevance to pathogenesis of neurodegenerative diseases", *ActaPharmacologicaSinica*, Vol. 30 (4), pp. 379-87.

Eisen, A. A., 2007, *Motor Neuron Disorders & Related Diseases: Handbook of Clinical Neurology*.

Elia, a J., T. L. Parkes, K. Kirby, P. St George-Hyslop, G. L. Boulianne, J. P. Phillips, and a J. Hilliker, 1999, "Expression of human FALS SOD in motorneurons of Drosophila", *Free Radical Biology & Medicine*, Vol. 26 (9-10), pp. 1332-8.

Elden, A. C. et al., 2010, "Ataxin-2 intermediate-length polyglutamine expansions are associated with increased risk for ALS", *Nature*, Vol. 466 (7310), pp. 1069-1075.

Elmore, T., R. Ignell, J. R. Carlson, and D. P. Smith, 2003, "Targeted mutation of a Drosophila odor receptor defines receptor requirement in a novel class of sensillum", *The Journal Of Neuroscience : The Official Journal Of The Society For Neuroscience*, Vol. 23 (30), pp. 9906-12.

Farooqui, T., and A. a Farooqui, 2009, "Aging: an important factor for the pathogenesis of neurodegenerative diseases", *Mechanisms Of Ageing And Development*, Vol. 130 (4), pp. 203-15.

Fernández-Santiago, R. et al., 2009, "Identification of novel Angiogenin (ANG) gene missense variants in German patients with amyotrophic lateral sclerosis.",*Journal Of Neurology*, Vol. 256 (8), pp. 1337-42.

Ghosh, S., and M. B. Feany, 2004, "Comparison of pathways controlling toxicity in the eye and brain in Drosophila models of human neurodegenerative diseases", *Human Molecular Genetics*, Vol. 13 (18), pp. 2011.

Gong, W. J., and K. G. Golic, 2003, "Ends-out, or replacement, gene targeting in Drosophila", *Proceedings Of The National Academy Of Sciences Of The United States Of America*, Vol. 100 (5), pp. 2556.

Gong, Y. H., a S. Parsadanian, a Andreeva, W. D. Snider, and J. L. Elliott, 2000, "Restricted expression of G86R Cu/Zn superoxide dismutase in astrocytes results in astrocytosis but does not cause motoneuron degeneration", *The Journal Of Neuroscience : The Official Journal Of The Society For Neuroscience*, Vol. 20 (2), pp. 660-5.

Gonzalez de Aguilar, J.-L., A. Echaniz-Laguna, A. Fergani, F. René, V. Meininger, J.-P. Loeffler, and L. Dupuis, 2007, "Amyotrophic lateral sclerosis: all roads lead to Rome", *Journal Of Neurochemistry*, Vol. 101 (5), pp. 1153-60.

Gordon, P. H. et al., 2007, "Efficacy of minocycline in patients with amyotrophic lateral sclerosis: a phase III randomised trial", *Lancet Neurology*, Vol. 6 (12), pp. 1045-53.

Greenway, M. J. et al., 2006, "ANG mutations segregate with familial and "sporadic" amyotrophic lateral sclerosis", *Nature Genetics*, Vol. 38 (4), pp. 411-3.

Gros-Louis, F. et al., 2008, "Als2 mRNA splicing variants detected in KO mice rescue severe motor dysfunction phenotype in Als2 knock-down zebrafish", *Human Molecular Genetics*, Vol. 17 (17), pp. 2691-702.

Gurney, M. E., H. Pu, a Y. Chiu, M. C. Dal Canto, C. Y. Polchow, D. D. Alexander, J. Caliendo, a Hentati, Y. W. Kwon, and H. X. Deng, 1994, "Motor neuron degeneration in mice that express a human Cu,Zn superoxide dismutase mutation", *Science (New York, N.Y.)*, Vol. 264 (5166), pp. 1772-5.

Hadano, S. et al., 2001, "A gene encoding a putative GTPase regulator is mutated in familial amyotrophic lateral sclerosis 2", *Nature Genetics*, Vol. 29 (2), pp. 166-73.

Hadano, S. et al., 2006, "Mice deficient in the Rab5 guanine nucleotide exchange factor ALS2/alsin exhibit age-dependent neurological deficits and altered endosome trafficking", *Human Molecular Genetics*, Vol. 15 (2), pp. 233-50.

Hall, E. D., J. aOostveen, and M. E. Gurney, 1998, "Relationship of microglial and astrocytic activation to disease onset and progression in a transgenic model of familial ALS", *Glia*, Vol. 23 (3), pp. 249-56.

Hanson, K. D., and J. M. Sedivy, 1995, "Analysis of biological selections for high-efficiency gene targeting", *Molecular And Cellular Biology*, Vol. 15 (1), pp. 45-51.

Hicks, G. G. et al., 2000, "Fus deficiency in mice results in defective B-lymphocyte development and activation, high levels of chromosomal instability and perinatal death", *Nature Genetics*, Vol. 24 (2), pp. 175-9.

Higgins, C. M. J., C. Jung, H. Ding, and Z. Xu, 2002, "Mutant Cu, Zn superoxide dismutase that causes motoneuron degeneration is present in mitochondria in the CNS", *The Journal Of Neuroscience : The Official Journal Of The Society For Neuroscience*, Vol. 22 (6), pp. RC215.

Hirth, F., 2010, "Drosophila melanogaster in the study of human neurodegeneration", *CNS &Neurological Disorders Drug Targets*, Vol. 9 (4), pp. 504-23.

Howland, D. S. et al., 2002, "Focal loss of the glutamate transporter EAAT2 in a transgenic rat model of SOD1 mutant-mediated amyotrophic lateral sclerosis (ALS)", *Proceedings Of The National Academy Of Sciences Of The United States Of America*, Vol. 99 (3), pp. 1604-9.

Ishigaki, S., N. Hishikawa, J.-ichiNiwa, S.-ichiroIemura, T. Natsume, S. Hori, A. Kakizuka, K. Tanaka, and G. Sobue, 2004, "Physical and functional interaction between Dorfin and Valosin-containing protein that are colocalized in ubiquitylated inclusions in neurodegenerative disorders.", *The Journal Of Biological Chemistry*, Vol. 279 (49), pp. 51376-85.

Jaarsma, D., F. Rognoni, W. van Duijn, H. W. Verspaget, E. D. Haasdijk, and J. C. Holstege, 2001, "CuZn superoxide dismutase (SOD1) accumulates in vacuolated

mitochondria in transgenic mice expressing amyotrophic lateral sclerosis-linked SOD1 mutations", *ActaNeuropathologica*, Vol. 102 (4), pp. 293–305.

Johnson, J. O. et al., 2010, "Exome sequencing reveals VCP mutations as a cause of familial ALS.",*Neuron*, Vol. 68 (5), pp. 857-64.

Julien, J.-P., 2007, "ALS: astrocytes move in as deadly neighbors", *Nature Neuroscience*, Vol. 10 (5), pp. 535-7.

Kabashi, E. et al., 2010, "Gain and loss of function of ALS-related mutations of TARDBP (TDP-43) cause motor deficits in vivo", *Human Molecular Genetics*, Vol. 19 (4), pp. 671-83.

Kato, S., M. Takikawa, K. Nakashima, a Hirano, D. W. Cleveland, H. Kusaka, N. Shibata, M. Kato, I. Nakano, and E. Ohama, 2000, "New consensus research on neuropathological aspects of familial amyotrophic lateral sclerosis with superoxide dismutase 1 (SOD1) gene mutations: inclusions containing SOD1 in neurons and astrocytes", *Amyotrophic Lateral Sclerosis And Other Motor Neuron Disorders : Official Publication Of The World Federation Of Neurology, Research Group On Motor Neuron Diseases*, Vol. 1 (3), pp. 163-84.

Kikuchi, H., G. Almer, S. Yamashita, C. Guégan, M. Nagai, Z. Xu, A. a Sosunov, G. M. McKhann, and S. Przedborski, 2006, "Spinal cord endoplasmic reticulum stress associated with a microsomal accumulation of mutant superoxide dismutase-1 in an ALS model", *Proceedings Of The National Academy Of Sciences Of The United States Of America*, Vol. 103 (15), pp. 6025-30.

Kraemer, B. C., T. Schuck, J. M. Wheeler, L. C. Robinson, J. Q. Trojanowski, V. M. Y. Lee, and G. D. Schellenberg, 2010, "Loss of murine TDP-43 disrupts motor function and plays an essential role in embryogenesis", *ActaNeuropathologica*, Vol. 119 (4), pp. 409-19.

Kuroda, M. et al., 2000, "Male sterility and enhanced radiation sensitivity in TLS(-/-) mice", *The EMBO journal*, Vol. 19 (3), pp. 453-62.

Kwiatkowski, T. J. et al., 2009, "Mutations in the FUS/TLS gene on chromosome 16 cause familial amyotrophic lateral sclerosis", *Science (New York, N.Y.)*, Vol. 323 (5918), pp. 1205-8.

Lai, C. et al., 2006, "Amyotrophic lateral sclerosis 2-deficiency leads to neuronal degeneration in amyotrophic lateral sclerosis through altered AMPA receptor trafficking", *The Journal Of Neuroscience : The Official Journal Of The Society For Neuroscience*, Vol. 26 (45), pp. 11798-806.

Lemmens, R., A. Van Hoecke, N. Hersmus, V. Geelen, I. D'Hollander, V. Thijs, L. Van Den Bosch, P. Carmeliet, and W. Robberecht, 2007, "Overexpression of mutant superoxide dismutase 1 causes a motor axonopathy in the zebrafish", *Human Molecular Genetics*, Vol. 16 (19), pp. 2359-65.

Li, Y., P. Ray, E. J. Rao, C. Shi, W. Guo, X. Chen, E. a Woodruff, K. Fushimi, and J. Y. Wu, 2010, "A Drosophila model for TDP-43 proteinopathy", *Proceedings Of The National Academy Of Sciences Of The United States Of America*, Vol. 107 (7), pp. 3169-74.

Lomen-Hoerth, C., 2008, "Amyotrophic lateral sclerosis from bench to bedside", *Seminars In Neurology*, Vol. 28 (2), pp. 205–211.

Lu, B., and H. Vogel, 2009, "Drosophila models of neurodegenerative diseases", *Annual Review Of Pathology*, Vol. 4, pp. 315-42.

Maruyama, H. et al., 2010, "Mutations of optineurin in amyotrophic lateral sclerosis", *Nature*, Vol. 465 (May)

Mitchell, J. D., and G. D. Borasio, 2007, "Amyotrophic lateral sclerosis", *Lancet*, Vol. 369 (9578), pp. 2031-41.

Mockett, R. J., S. N. Radyuk, J. J. Benes, W. C. Orr, and R. S. Sohal, 2003, "Phenotypic effects of familial amyotrophic lateral sclerosis mutant Sod alleles in transgenic Drosophila", *Proceedings Of The National Academy Of Sciences Of The United States Of America*, Vol. 100 (1), pp. 301-6.

Murakami, T., I. Nagano, T. Hayashi, Y. Manabe, M. Shoji, Y. Setoguchi, and K. Abe, 2001, "Impaired retrograde axonal transport of adenovirus-mediated E. coli LacZ gene in the mice carrying mutant SOD1 gene", *Neuroscience Letters*, Vol. 308 (3), pp. 149-52.

Murray, C. A., 2006, *AmyotrophicLateral Sclerosis: New Research*, Nova Science Pub Inc.

Nagai, M., M. Aoki, I. Miyoshi, M. Kato, P. Pasinelli, N. Kasai, R. H. Brown, and Y. Itoyama, 2001, "Rats expressing human cytosolic copper-zinc superoxide dismutase transgenes with amyotrophic lateral sclerosis: associated mutations develop motor neuron disease", *The Journal Of Neuroscience : The Official Journal Of The Society For Neuroscience*, Vol. 21 (23), pp. 9246-54.

Nassif, M., S. Matus, K. Castillo, and C. Hetz, 2010, "Amyotrophic lateral sclerosis pathogenesis: a journey through the secretory pathway", *Antioxidants & Redox Signaling*, Vol. 13 (12), pp. 1955-89.

Nishimura, A. L. et al., 2004, "A mutation in the vesicle-trafficking protein VAPB causes late-onset spinal muscular atrophy and amyotrophic lateral sclerosis", *American journal of human genetics*, Vol. 75 (5), pp. 822-31.

Okado-Matsumoto, A., and I. Fridovich, 2001, "Subcellular distribution of superoxide dismutases (SOD) in rat liver: Cu,Zn-SOD in mitochondria", *The Journal of Biological Chemistry*, Vol. 276 (42), pp. 38388-93.

Orlacchio, A. et al., 2010, "SPATACSIN mutations cause autosomal recessive juvenile amyotrophic lateral sclerosis", *Brain : A Journal Of Neurology*, Vol. 133 (Pt 2), pp. 591-8.

Oztug Durer, Z. a et al., 2009, "Loss of metal ions, disulfide reduction and mutations related to familial ALS promote formation of amyloid-like aggregates from superoxide dismutase", *PloS One*, Vol. 4 (3), pp. e5004.

Parkes, T. L., A. J. Elia, D. Dickinson, A. J. Hilliker, J. P. Phillips, and G. L. Boulianne, 1998, "Extension of Drosophila lifespan by overexpression of human SOD1 in motorneurons", *Nature Genetics*, Vol. 19 (2), pp. 171-174.

Pasinelli, P., D. R. Borchelt, M. K. Houseweart, D. W. Cleveland, and R. H. Brown, 1998, "Caspase-1 is activated in neural cells and tissue with amyotrophic lateral sclerosis-associated mutations in copper-zinc superoxide dismutase", *Proceedings Of The National Academy Of Sciences Of The United States Of America*, Vol. 95 (26), pp. 15763-8.

Pasinelli, P., and R. H. Brown, 2006, "Molecular biology of amyotrophic lateral sclerosis: insights from genetics", *Nature Reviews. Neuroscience*, Vol. 7 (9), pp. 710-23.

Pramatarova, a, J. Laganière, J. Roussel, K. Brisebois, and G. a Rouleau, 2001, "Neuron-specific expression of mutant superoxide dismutase 1 in transgenic mice does not lead to motor impairment", *The Journal Of Neuroscience : The Official Journal Of The Society For Neuroscience*, Vol. 21 (10), pp. 3369-74.

Puls, I. et al., 2003, "Mutant dynactin in motor neuron disease", *Nature Genetics*, Vol. 33 (4), pp. 455-6.

Rakhit, R., J. P. Crow, J. R. Lepock, L. H. Kondejewski, N. R. Cashman, and A. Chakrabartty, 2004, "Monomeric Cu,Zn-superoxide dismutase is a common misfolding intermediate in the oxidation models of sporadic and familial amyotrophic lateral sclerosis", *The Journal Of Biological Chemistry*, Vol. 279 (15), pp. 15499-504.

Rakhit, R., P. Cunningham, A. Furtos-Matei, S. Dahan, X.-F. Qi, J. P. Crow, N. R. Cashman, L. H. Kondejewski, and A. Chakrabartty, 2002, "Oxidation-induced misfolding and aggregation of superoxide dismutase and its implications for amyotrophic lateral sclerosis", *The Journal Of Biological Chemistry*, Vol. 277 (49), pp. 47551-6.

Reiter, L. T., L. Potocki, S. Chien, M. Gribskov, and E. Bier, 2001, "A systematic analysis of human disease-associated gene sequences in Drosophila melanogaster", *Genome Research*, Vol. 11 (6), pp. 1114-25.

Rong, Y. S., and K. G. Golic, 2001, "A targeted gene knockout in Drosophila", *Genetics*, Vol. 157 (3), pp. 1307-12.

Rong, Y. S., 2000, "Gene Targeting by Homologous Recombination in Drosophila", *Science*, Vol. 288 (5473), pp. 2013-2018.

Rosen, D. R., T. Siddique, D. Patterson, D. A. Figlewicz, P. Sapp, A. Hentati, D. Donaldson, J. Goto, J. P. O'Regan, and H. X. Deng, 1993, "Mutations in Cu/Zn superoxide dismutase gene are associated with familial amyotrophic lateral sclerosis", *Nature*, Vol. 362 (6415), pp. 59–62.

Ross, C. a, and M. a Poirier, 2004, "Protein aggregation and neurodegenerative disease", *Nature Medicine*, Vol. 10 Suppl (July), pp. S10-7.

Rothstein, J. D., 2009, "Current hypotheses for the underlying biology of amyotrophic lateral sclerosis", *Annals Of Neurology*, Vol. 65 Suppl 1, pp. S3-9.

Roy, S., B. Zhang, V. M.-Y. Lee, and J. Q. Trojanowski, 2005, "Axonal transport defects: a common theme in neurodegenerative diseases", *ActaNeuropathologica*, Vol. 109 (1), pp. 5-13.

Sabatelli, M., F. Madia, a Conte, M. Luigetti, M. Zollino, I. Mancuso, M. Lo Monaco, G. Lippi, and P. Tonali, 2008, "Natural history of young-adult amyotrophic lateral sclerosis", *Neurology*, Vol. 71 (12), pp. 876-81.

Salinas, S., C. Proukakis, A. Crosby, and T. T. Warner, 2008, "Hereditary spastic paraplegia: clinical features and pathogenetic mechanisms", *Lancet Neurology*, Vol. 7 (12), pp. 1127-38.

Sathasivam, S., 2010, "Motor neurone disease: clinical features, diagnosis, diagnostic pitfalls and prognostic markers", *Singapore Medical Journal*, Vol. 51 (5), pp. 367-72; quiz 373.

Shi, P., J. Gal, D. M. Kwinter, X. Liu, and H. Zhu, 2010, "Mitochondrial dysfunction in amyotrophic lateral sclerosis", *Biochimica Et BiophysicaActa*, Vol. 1802 (1), pp. 45-51.

Shulman, J. M., L. M. Shulman, W. J. Weiner, and M. B. Feany, 2003, "From fruit fly to bedside: translating lessons from Drosophila models of neurodegenerative disease", *Current Opinion In Neurology*, Vol. 16 (4), pp. 443-9.

Siddique, T., D. A. Figlewigz, M. A. Pericak-Vance, J. L. Haines, G. Rouleau, A. J. Jeffers, P. Sapp, W. Y. Hung, J. Bebout, and D. McKenna-Yasek, 1991, "Linkage of a gene causing familial amyotrophic lateral sclerosis to chrosome 21 and evidence of genetic locus heterogeneity", *New England Journal Of Medicine*, Vol. 324 (20), pp. 1381–1384.

Smith, B. D., and R. T. Raines, 2006, "Genetic selection for critical residues in ribonucleases", *Journal Of Molecular Biology*, Vol. 362 (3), pp. 459-78.

Sreedharan, J. et al., 2008, "TDP-43 mutations in familial and sporadic amyotrophic lateral sclerosis", *Science*, Vol. 319 (5870), pp. 1668-72.

Staber, C. et al., 2011, "Perturbing A-to-I RNA Editing Using Genetics and Homologous Recombination", Methods In Molecular Biology, vol. 718, pp. 41-73.

Subramaniam, J. R., W. E. Lyons, J. Liu, T. B. Bartnikas, J. Rothstein, D. L. Price, D. W. Cleveland, J. D. Gitlin, and P. C. Wong, 2002, "Mutant SOD1 causes motor neuron disease independent of copper chaperone-mediated copper loading", *Nature Neuroscience*, Vol. 5 (4), pp. 301-7.

Suraweera, A. et al., 2007, "Senataxin, defective in ataxia oculomotor apraxia type 2, is involved in the defense against oxidative DNA damage", *The Journal Of Cell Biology*, Vol. 177 (6), pp. 969-79.

Suzuki, H., K. Kanekura, T. P. Levine, K. Kohno, V. M. Olkkonen, S. Aiso, and M. Matsuoka, 2009, "ALS-linked P56S-VAPB, an aggregated loss-of-function mutant of VAPB, predisposes motor neurons to ER stress-related death by inducing aggregation of co-expressed wild-type VAPB", *Journal Of Neurochemistry*, Vol. 108 (4), pp. 973-985.

Tateno, M. et al., 2004, "Calcium-permeable AMPA receptors promote misfolding of mutant SOD1 protein and development of amyotrophic lateral sclerosis in a transgenic mouse model", *Human Molecular Genetics*, Vol. 13 (19), pp. 2183-96.

Ticozzi, N., C. Tiloca, C. Morelli, C. Colombrita, B. Poletti, A. Doretti, L. Maderna, S. Messina, A. Ratti, and V. Silani, 2011, "Genetics of familial amyotrophic lateral sclerosis", *Archives Italiennes De Biologie*, Vol. 149 (1), pp. 65-82.

Trotti, D., a Rolfs, N. Danbolt, R. Brown, and M. Hediger, 1999, "SOD1 mutants linked to amyotrophic lateral sclerosis selectively inactivate a glial glutamate transporter", *Nature Neuroscience*, Vol. 2 (9), pp. 848.

Tsuda, H. et al., 2008, "The amyotrophic lateral sclerosis 8 protein VAPB is cleaved, secreted, and acts as a ligand for Eph receptors", *Cell*, Vol. 133 (6), pp. 963-77.

Uversky, V., 2007, *Protein Misfolding, Aggregation and Conformational Diseases: Part B: Molecular Mechanisms of Conformational Diseases*.

Valdmanis, P. N., and G. a Rouleau, 2008, "Genetics of familial amyotrophic lateral sclerosis", *Neurology*, Vol. 70 (2), pp. 144-52.

Valentine, J. S., P. a Doucette, and S. Zittin Potter, 2005, "Copper-zinc superoxide dismutase and amyotrophic lateral sclerosis", *Annual Review Of Biochemistry*, Vol. 74, pp. 563-93.

Van Damme, P., D. Braeken, G. Callewaert, W. Robberecht, and L. Van Den Bosch, 2005, "GluR2 deficiency accelerates motor neuron degeneration in a mouse model of amyotrophic lateral sclerosis", *Journal Of Neuropathology &Experimental Neurology*, Vol. 64 (7), pp. 605.

Van Den Bosch, L., 2011, "Genetic Rodent Models of Amyotrophic Lateral Sclerosis", *Journal Of Biomedicine And Biotechnology*, Vol. 2011 (348765)

Vukosavic, S., L. Stefanis, V. Jackson-Lewis, C. Guégan, N. Romero, C. Chen, M. Dubois-Dauphin, and S. Przedborski, 2000, "Delaying caspase activation by Bcl-2: A clue to disease retardation in a transgenic mouse model of amyotrophic lateral

sclerosis", *The Journal Of Neuroscience : The Official Journal Of The Society For Neuroscience*, Vol. 20 (24), pp. 9119-25.

Wang, J., G. W. Farr, D. H. Hall, F. Li, K. Furtak, L. Dreier, and A. L. Horwich, 2009, "An ALS-linked mutant SOD1 produces a locomotor defect associated with aggregation and synaptic dysfunction when expressed in neurons of Caenorhabditiselegans", *PLoS Genetics*, Vol. 5 (1), pp. e1000350.

Watson, M. R., R. D. Lagow, K. Xu, B. Zhang, and N. M. Bonini, 2008, "A drosophila model for amyotrophic lateral sclerosis reveals motor neuron damage by human SOD1", *The Journal Of Biological Chemistry*, Vol. 283 (36), pp. 24972-81.

Williamson, T. L., and D. W. Cleveland, 1999, "Slowing of axonal transport is a very early event in the toxicity of ALS-linked SOD1 mutants to motor neurons", *Nature Neuroscience*, Vol. 2 (1), pp. 50-6.

Witan, H., A. Kern, I. Koziollek-Drechsler, R. Wade, C. Behl, and A. M. Clement, 2008, "Heterodimer formation of wild-type and amyotrophic lateral sclerosis-causing mutant Cu/Zn-superoxide dismutase induces toxicity independent of protein aggregation", *Human Molecular Genetics*, Vol. 17 (10), pp. 1373-85.

Wu, D.-C., D. B. Ré, M. Nagai, H. Ischiropoulos, and S. Przedborski, 2006, "The inflammatory NADPH oxidase enzyme modulates motor neuron degeneration in amyotrophic lateral sclerosis mice", *Proceedings Of The National Academy Of Sciences Of The United States Of America*, Vol. 103 (32), pp. 12132-7.

Xu, Z., L. C. Cork, J. W. Griffin, and D. W. Cleveland, 1993, "Increased expression of neurofilament subunit NF-L produces morphological alterations that resemble the pathology of human motor neuron disease", *Cell*, Vol. 73 (1), pp. 23-33.

Yamanaka, K., T. M. Miller, M. McAlonis-Downes, S. J. Chun, and D. W. Cleveland, 2006, "Progressive spinal axonal degeneration and slowness in ALS2-deficient mice", *Annals Of Neurology*, Vol. 60 (1), pp. 95-104.

Yu, Z., and R. Jiao, 2010, "Advances in Drosophila gene targeting and related techniques", *Frontiers in Biology*, Vol. 5 (3), pp. 238–245.

Zhang, B., P. Tu, F. Abtahian, J. Q. Trojanowski, and V. M. Lee, 1997, "Neurofilaments and orthograde transport are reduced in ventral root axons of transgenic mice that express human SOD1 with a G93A mutation", *The Journal Of Cell Biology*, Vol. 139 (5), pp. 1307-15.